AN INVESTIGATION OF PRESSURE DROP IN A TWO-PHASE TWO-COMPONENT FLOW IN BENDS

by

MELVIN I. COHEN

Submitted in Partial Fulfillment of the
Requirements for the Degree of
Bachelor of Science
at the
Massachusetts Institute of Technology
June, 1957

Signature of Author _____
Department of Mechanical Engineering,
May 20, 1957

Certified by _____
Thesis Supervisor

Accepted by _____
Chairman, Departmental Committee on
Undergraduate Students

Cambridge, Massachusetts

May 20, 1957

Professor L. F. Hamilton
Secretary of the Faculty
Massachusetts Institute of Technology
Cambridge, Massachusetts

Dear Professor Hamilton:

In partial fulfillment of the requirements for the degree of Bachelor of Science in Mechanical Engineering, I hereby submit my thesis entitled, "An Investigation of Pressure Drop in a Two-Phase Two-Component Flow in Bends".

Very truly yours,

Melvin I. Cohen

ACKNOWLEDGEMENT

This project could not have been undertaken without the cooperation of Mr. J. Castillo who developed the theory of two-phase bend losses used herein and the Babcock and Wilcox Company who provided financial assistance.

The author gratefully acknowledges the advice, assistance and close cooperation given him by Professor M. A. Santalo.

TABLE OF CONTENTS

TABLE OF CONTENTS (CONT.)

ABSTRACT

"An Investigation of Pressure Drop in a Two-Phase Two-Component Flow in Bends"

by

Melvin I. Cohen

The increased utilization of two-phase flow by industry in recent years has led to a great deal of investigation and analysis of the pressure drop of two-phase flow in pipes. Although much work has been done with straight pipes the nature of the two-phase pressure drop in pipe bends is virtually unknown.

It was the purpose of this investigation to provide organized data for two-phase bend pressure drop which could be presented as a non-dimensional correlation to facilitate the design of two-phase piping systems. An apparatus was constructed on which could be investigated two-phase and water flow for both straight pipe and 90° bends. By means of a direct comparison with straight pipe correlations, it was predicted that the ratio of the two-phase bend pressure drop to the single-phase pressure drop in bends would also depend only on the flow quality and the bend radius.

The results of this investigation for three different bends are the following:

1. The above predicted relationship was seen to be valid for the bends tested;

2. The ratio of two-phase to single-phase pressure drop in a bend was seen to be different than the corresponding straight pipe ratio, depending on the bend radius;

3. The ratio of total two-phase bend pressure drop to that due only to friction was found to be a function only of the relative radius of the bend. For very sharp bends this ratio was a great deal higher than that for a flow of water alone.

I INTRODUCTION

In recent years a great deal of practical interest has arisen in the co-current flow in pipes of a liquid and a gas. The petroleum industry makes wide use of two-phase flow both in air-lift pumps to drain underground oil pools and in the simultaneous pipe line transmission of oil and natural gas. Chemical process equipment very often requires a charge of previously mixed vapor and gas to feed a reaction and, more recently, the nuclear power industry has begun using evaporating liquids to cool reactors. The production of steam in modern, coil-type boilers, finally provides still another wide spread application of two-phase flow.

In order to effectively design a two-phase piping system it is necessary for the designer to know the pressure drop that will occur within the pipe for various flow conditions. A great deal of data is available on two-phase flow in straight pipes and investigators have, to a large extent, been able to group this data in general, non-dimensional plots and correlate them with their own analytical predictions and explanations. The designer has only to tap this wealth of information and apply it to his specific case.

The procedure is not so simple, however in the case of a curved pipe. Experience has shown that pressure losses in curved pipes for two-phase flow as well as for water flow are usually significantly higher than those for the

corresponding flow in a straight pipe. Although sufficient data is available in curved pipe pressure drop in single-phase flow to facilitate design the corresponding problem in two-phase flow has never, to the best of the author's knowledge, been investigated. Practically, such a situation is quite common, arising in flow around 90° pipe bends and boiler coils.

The author's purpose in undertaking this investigation was to provide organized experimental data concerning pressure losses in an adiabatic flow of a mixture of water and air around various 90° pipe bends. It was hoped that such data could be compared with that for water alone and serve as a basis for predicting bend pressure drops for the co-current flow of any liquid and gas.

II BACKGROUND MATERIAL

A great deal of experimental and analytical work has been done on the nature of pressure drop in straight pipes for two-phase flow and on single-phase pressure drops in pipe bends. Since this material will later provide the basis for predicting the nature of two-phase pressure drops in bends the results of some of these investigations will be discussed.

2.1 Straight Pipe

Baker (1) has explained that the increase in pressure drop of a liquid flowing in a straight pipe when a gas is introduced is due mainly to the following reasons:
(1) Many authors have found that the gas flows a great deal faster than does the liquid. This phenomenon of slip between the two phases creates friction within the flow in addition to the usual pipe friction. An increase in pressure drop must supply this increased dissipation of energy.
(2) As air is introduced into the pipe the crossectional area of flow available to the water is decreased. Additional pressure drop is obtained because of one phase interfering with the flow of the other.

Baker observed that, depending upon the mass flow rates and densities of the components, various geometrical flow regimes or patterns could be obtained. Most important among these are separated flow in which the gas flows above

the liquid with either a laminar (stratified) or a wavy interface between them, annular flow in which the liquid forms an annulus about the inside of the pipe, the gas flowing as a core through the middle, and a fog-type flow in which the liquid forms tiny droplets in the gas.

Martinelli et al. (2) obtained a large amount of experimental data for the adiabatic flow of two phases in a horizontal pipe. They found a significant influence of the slip on the pressure drop but no significant effect due to the geometrical pattern of the phases. They hypothesized that the pressure drop of the liquid phase and that of the gas phase were both equal to the pressure drop of the mixture. Applying the Fanning equation to each phase leads to:

$$\left(\frac{dp}{dL}\right)_{TP} = \phi_L \frac{\rho_L}{D_L} \frac{V_L^2}{2g} \qquad (1\text{ a})$$

$$\left(\frac{dp}{dL}\right)_{TP} = \phi_G \frac{\rho_G}{D_G} \frac{V_L^2}{2g} \qquad (1\text{ b})$$

D_L and D_G are the hydraulic diameters of the liquid and gas phases, and are related to the mass flows through two empirical parameters α and β,

$$V_L = \frac{w_L}{\alpha\left(\frac{\pi}{4} D_L^2\right)\rho_L} \qquad (1\text{ c})$$

$$(V_G) = \frac{W_G}{\beta\left(\frac{\pi}{4} D_G^2\right)\rho_G} \qquad (1\,d)$$

If it is further assumed that the gas phase always has a circular cross-section, then $\beta = 1$. Any actual departure from this idealized condition will reflect on a variation of α.

The friction factor in equation (5) may be assumed to be on the general form

$$\phi = \frac{K}{\left(\frac{\rho V D}{\mu}\right)^m} = \frac{K}{\left(\frac{GD}{\mu}\right)^m} = \left(\frac{\pi}{4}\right)^m \frac{K}{\left(\frac{w}{\mu D}\right)^m} \qquad (2)$$

Martinelli distinguishes four different cases in this equation:

(a) Both liquid and gas flows are turbulent, $k_g = k = 0.184$, $m_g = m = 0.2$ (Reynolds numbers between 5000 and 200,000).

(b) Both the liquid and gas flows are viscous, $k_g = k = 64$, $m_g = m = 1$.

(c) The gas is turbulent and the liquid is viscous, $k_g = 0.184$, $k_g = 64$, $m_g = 0.2$, $m = 1$.

(d) The gas is viscous and the liquid is turbulent, $k_g = 64$, $k = 0.184$, $m_g = 1$, $m = 0.2$.

The last case is very improbable and of the other three the first is the most important and will be the only one analyzed here.

For convenience in nomenclature he introduces two fictitious terms. These turn out to be the pressure drop that would occur if only the gas phase of the liquid phase would flow in the pipe, the other phase not being present. From the Fanning equation and equation (2) with m = 0.2 and k = 0.184, these terms become by definition:

$$\left(\frac{\Delta P}{\Delta L}\right)_L \equiv \phi_L' \frac{\rho_L}{D} \frac{\left(w_L/\rho_L \frac{\pi}{4} D^2\right)^2}{2g} = \frac{0.184\, \mu_L^{0.2}\, w_L^{1.8}}{\left(\frac{\pi}{4}\right)^{1.8} D^{4.8}\, \rho_L\, 2g} \qquad (3\,a)$$

and similarly

$$\left(\frac{\Delta P}{\Delta L}\right)_G \equiv \frac{0.184\, \mu_G^{0.2}\, w_G^{1.8}}{\left(\frac{\pi}{4}\right)^{1.8} D^{4.8}\, \rho_G\, 2g} \qquad (3\,b)$$

where D is now the diameter of the pipe. For a given pipe these two terms can be evaluated knowing the properties of the fluids, the total flow rate and the quality of the mixture. Since the total volume of the pipe is the sum of the volumes occupied by each phase, per unit length of pipe,

$$\alpha\left(\frac{\pi}{4} D_L^2\right) + \frac{\pi}{4} D_G^2 = \frac{\pi}{4} D^2 \qquad (4)$$

Equations (1) through (4) are sufficient to express D_L, D_g, V_L, V_g or the desired $(\Delta p/\Delta L)_{TP}$ in terms of the quantities (3 a) and (3 b) and the unknown parameter α. To evaluate the pressure drop the combination of these equations results in:

$$\left(\frac{\Delta P}{\Delta L}\right)_{TP} = \left(\frac{\Delta P}{\Delta L}\right)_G \left(\frac{D}{D_G}\right)^{4.8}$$

$$= \left(\frac{\Delta P}{\Delta L}\right)_G \left[1 + \alpha^{1/4} \times^{0.833}\right]^{2.4}$$

(5)

where

$$X^2 = \frac{(\Delta P/\Delta L)_L}{(\Delta P/\Delta L)_G} = \left(\frac{\mu_L}{\mu_G}\right)^{0.2} \left(\frac{\rho_G}{\rho_L}\right)\left(\frac{w_L}{w_G}\right)^{1.8}$$

(6)

It was found experimentally that, at least for a horizontal pipe, α could be correlated with X alone, so that

$$\Phi^2_{G_{TT}} = \frac{(\Delta P/\Delta L)_{TP}}{(\Delta P/\Delta L)_G} = f(X)$$

(7 a)

and similarly

$$\Phi^2_{L_{TT}} = \frac{(\Delta P/\Delta L)_{TP}}{(\Delta P/\Delta L)_L} = f(X)$$

(7 b)

Martinelli further found experimentally that the ratio of the two-phase pressure drop to the pressure drop that would occur if the liquid alone were flowing with a mass flow equal to the total two-phase mass flow, $(\Delta P/\Delta L)_o$, was also a function only of X. For small changes in temperature and pressure the viscosity and pressure ratios in equation (6) become constant and X becomes a function only of the flow quality. The final result--for pressure drops small enough to render the gas phase incompressible--may be written as:

$$\frac{(\Delta P/\Delta L)_{TP}}{(\Delta P/\Delta L)_o} = \phi(x) \qquad (7\,c)$$

In a later paper, Martinelli found that these results were not valid for critical temperature, pressure, viscosity or density ratio, so he modified them to take into account these parameters.

2.2 Single-phase Flow in a Bend

Beij (3) has thoroughly investigated the pressure drop in a flow of water around 90° pipe bends. He postulated that the total bend loss is a sum of three individual components; the pressure drop due to pipe friction, the pressure loss due to fluid particles being accelerated and decelerated by the centrifugal field in the bend and, finally, the pressure drop that occurs in the section of pipe downstream of the bend as a result of the damping out of turbulent effects initiated by the bend. Beij states that since each of these terms is a

dynamic effect dimensional analysis predicts that they will be proportional to $\frac{V^2}{2g}$:

$$\frac{\Delta P_B}{\rho_w g} = \left(f \frac{L}{D} + n + \epsilon \right) \frac{V^2}{2g} \qquad (8)$$

where:

f is the Fanning friction factor,

n , ϵ are terms relating to the acceleration and turbulence losses, and

L is the axial length of the bend.

If n and ϵ are absorbed in one coefficient, η , the term, $\eta \frac{V^2}{2g}$ may be interpreted as that part of the total bend loss which is due to factors other than pipe friction. Throughout this paper this term will be called the <u>secondary bend loss</u>, ΔP_S.

The results of Beij's experimental work show that the fraction of the total bend loss that is due to secondary effects is a function only of the <u>relative radius</u> of the bend: R/D, where R is the bend radius and D the pipe diameter. These results are shown in figure 1. <u>Equivalent length</u> is only the length of straight pipe that would produce the same total pressure loss as the bend.

It is interesting to note that at an R/D of 1 ΔP_S is much greater than the frictional loss and at R/D of 6 and greater the secondary losses become small when compared with

those due to friction. At an R/D of 3 or 4 the secondary pressure loss is about equal to the frictional pressure loss.

III ANALYSIS OF TWO-PHASE FLOW IN BENDS

3.1 Extension of the Martinelli Analysis to the Flow in Bends

Rather than actually conducting an analysis of two-phase flow in bends, the author felt that an attempt at correlating the two-phase bend pressure drop with other flow parameters by a direct comparison with the Martinelli correlation for straight pipes would yield a much more practical result. Since the usefulness of such a correlation has already been proved in straight-pipe design, the extension of it to curved pipes would provide the two-phase pipe designer with an ever more powerful tool. Knowing only the quality of the flow and the pressure drop that would occur in a flow of water alone, he could successfully predict the two-phase pressure drop.

By basing his analysis of two-phase flow on the Fanning equation Martinelli assumed that the pressure drop was a dynamic effect of the flow, proportional to the square of the velocities of the individual phases. Since Beij showed that the bend pressure loss was also a dynamic term it is expected that a relationship of the same sort as equation 7 will hold in two-phase flow around a bend for both the total and secondary bend pressure drops.

3.2 Analytical Approach to the Problem

Castillo (4) has postulated that most of the secondary bend loss in stratified two-phase flow is due to the rotation

of the fluids in a plane perpendicular to the bend axis and to the centrifugal effect of the two fluids separating as the lighter gas tends to move to the inside of the bend. Since this latter term is not present in single-phase flow it is expected that values of bend pressure ratio will be higher than those predicted by Martinelli for a straight pipe.

To evaluate the losses due to rotation a section of fluid of infinitesimal thickness in the direction of the flow is assumed to move as a solid body. The rotation about the bend axis is due primarily to the effect of the centrifugal field, friction between the liquid and the pipe and between two consecutive sections of fluid being neglected.

Consider a portion of liquid of mass dm whose centroid is a distance, a, away from the center of the pipe (see diagram).

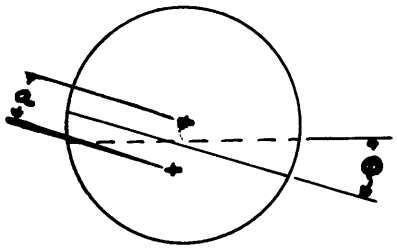

Newton's equation yields a relation between the angle of rotation, φ, and the time that has elapsed since the fluid entered the bend:

$$dm \frac{V_i^2}{R} a \cos\varphi - dm g a \sin\varphi = dm K_0^2 \frac{d^2\varphi}{dt^2}$$

where K_0 is the radius of gyration of the liquid model, R

the mean bend radius and V_L is the liquid velocity.

By assuming small angles of rotation a modified form of the above equation may be written:

$$\frac{d^2\varphi}{d\tau^2} + \frac{g\,a}{\kappa_0^2}\,\varphi = \frac{V_L^2\,a}{R\,\kappa_0^2} \qquad (10\,a)$$

With the boundary conditions, $\varphi = 0$ and $\frac{d\varphi}{d\tau} = 0$ at $\tau = 0$ the solution to this equation is:

$$\varphi = \frac{V_L^2}{Rg}\left(1 - \cos\sqrt{g\,a/\kappa_0^2}\;\tau\right) \qquad (11)$$

As the kinetic energy of the fluid increases due to rotation the pressure of the fluid must decrease according to Bernoulli's equation. In the absence of friction the pressure variation would be sinusoidal in time. The presence of friction will damp the oscillation and produce a net pressure drop which, for simplicity, may be assumed to equal the maximum kinetic energy due to rotation. From the above equation,

$$\frac{1}{2}\,\frac{\kappa_0^2}{g}\left(\frac{d\varphi}{d\tau}\right)^2 = \frac{1}{2}\left(\frac{V_L^2}{Rg}\right) a \sin^2 K\tau \qquad (12)$$

which has a maximum

$$\frac{\Delta P_{MAX}}{\rho} = \frac{1}{2}\left(\frac{V_L^2}{Rg}\right) a \qquad (12a)$$

The dimension, a, is a unique function of A_L, the cross sectional area of the liquid flow. It can be related to flow rates through continuity

$$\rho_L V_L A_L = w_L, \quad \rho_G V_G (A - A_L) = w_G$$

and some knowledge on the velocity ratio between the gas and liquid V_G / V_L . Castillo has obtained an exact solution of equation 10 in the form of an elliptic integral and from this more accurately calculated the energy dissipation and the pressure drop. Figure 21 shows the exact solution for a bend with R/D equal to 1 plotted in the form of the Martinelli relationship. For the empirical assumption that $V_G / V_L = (\rho_L / \rho_G)^{1/3}$. Although this plot represents only rotational losses in a separated flow it is significant in that it does analytically predict a correlation of the Martinelli type for bend losses.

3.3 Experimental Program

In order to verify these predictions an apparatus was constructed in which could be produced a flow of a two-phase mixture both in a straight pipe and in a 90° bend. Provision was made for the measurement of both the fluid flows and the pressure at various points along the straight and bent sections. By means of this arrangement it was possible to measure the single-and two-phase pressure drops for various flow qualities.

Since an investigation into the nature of the two-phase flow in pipe bends would be the first of its kind the fluids considered should be simple in nature. A mixture of air and water would serve this purpose because much data is available on the flow properties of these two fluids alone and they are

relatively easy to obtain and handle. Since the two phases are of different components the problem of mass transfer from one phase to another by condensation or evaporation is eliminated and the amount of each phase flowing at any time may be accurately measured.

IV APPARATUS AND TEST PROCEDURE

4.1 Apparatus Description

In order to carry out the desired investigation the experimental apparatus shown in figure 3 was constructed. A schematic diagram of the system (figure 4) indicates that it is composed of four sections, mixing, entry, test and exit, each of which performs a specific function.

In the mixing section the water and air are brought from their sources, their mass rates of flow measured by nozzles installed in the individual pipes and are finally mixed and introduced into the entry pipe. Water was obtained from the city water line and the air flow from a two-cylinder Joy compressor located in the Massachusetts Institute of Technology Steam Laboratory, which was able to deliver air at essentially constant temperature and any desired pressure up to 250 psig. Mixing was accomplished in a jet-type steam ejector (figure 5) in which a jet of air was introduced into the center of a flow of water. This type of mixer was used because it facilitated obtaining a fairly steady stratified flow, relatively free from disturbances. Originally, mixing was attempted in a common pipe "tee" connection but it was nearly impossible to obtain a stratified flow under these conditions. It will later be shown that although the use of the steam ejector gave a fairly good stratified flow it introduced a great deal of turbulence into the flow at higher velocities.

The entry region consists of $4\frac{1}{2}$ feet of 1/16 inch thick, 3/4 inch outside diameter clear lucite pipe attached to the mixer ot one end and the test section at the other by plexiglass flanges bonded to the pipe. It is the function of this section to provide enough straight pipe to allow the flow to develop fully and any turbulence introduced during mixing to die out before the flow enters the test section. A great deal of care was exhibited in connecting the entry pipe to the test section in order to assure accurate alignment of the pipes and the absence of edying in the flanged region. Pressure taps of .040" diameter were placed every 12 inches along the length of straight pipe.

The test section (figure 6) consisted of a 90° bend of clear lucite to which were fitted flanges at either end. It was easily removed by loosening the flange bolts in order to allow the investigation of more than one bend. Reference to the Beij curves, figure 1, indicates that for water a bend with a relative radius of 6 exhibits a pressure drop that is almost completely due to pipe friction, one with R/D equal to 4 shows frictional and secondary losses that are almost equal in magnitude and a bend with R/D of 1 attributes almost all of its pressure drop to secondary effects. It is for these reasons that the three test sections were constructed with relative radii of 1, 4 and 6.

Three feet of straight pipe fitted with two more pressure taps comprised the exit section. It is in this region

that disturbances of the flow due to the bend may be damped out before a final reading of the pressure is taken. At the outlet of the pipe is installed a gate valve by means of which the pressure in the entire apparatus may be controlled. The whole setup was quite level and after the mixer all piping was in a horizontal plane.

In order to measure the air and water flow rates standard A.S.M.E. flow nozzles were installed in the individual fluid lines before the mixer. Pressure drop along the pipes and bend were measured by connecting manometers to the pressure taps. This instrumentation is discussed in fuller detail in Appendix 1.

4.2 Test Procedure

4.21 Tests Performed With Water Only

As a check on the performance of the apparatus as a whole for a flow of water the pressure drop per unit length of straight pipe, $\frac{\Delta P}{\Delta L}$, was measured in the entry section, the pipe friction factor, f, calculated, and the friction factor plotted against Reynolds number.

$\frac{\Delta P}{\Delta L}$ was found by measuring the pressure difference between pressure taps 3 and 4 and dividing this by the distance between these taps. Taps 3 and 4 were used because it was felt that since they were toward the end of the entry section and a maximum distance away from the mixer they would give more accurate results than any other two pressure taps and that

their pressure difference would be due only to pipe friction. The results of this investigation were substituted into the Fanning friction equation,

$$\Delta P = f \frac{L}{D} \frac{V^2}{2g} \qquad (9)$$

and the corresponding friction factors calculated. The values of f and Reynolds number for various flows are tabulated in table I and plotted in figure 11, in which they are compared to the Moody curves. At low Reynolds number the friction factor lies on the Moody curve for a very rough pipe but at R_e equal to 5×10^5 a transition is made to the curve for a smooth pipe. The only possible explanation of this phenomenon is that the mixer imparts a great deal of turbulence to the flow until a Reynolds Number of 5×10^5 is reached. At this point the turbulence dies out before it reaches the third pressure tap and the normal friction factor-Reynolds number relationship for a smooth lucite pipe is obtained. Since all the data used in later calculations yielded Reynolds numbers below the critical value, the effect of this transition does not appear in any of the calculated results and the curve for a rough pipe was used to represent the flow.

Since it is assumed that the total pressure loss in the bend and the secondary bend loss are proportional to V^2 (eq. 8), it was felt that verification of this relationship would serve as another check on the setup's performance.

The total bend loss, ΔP_b, was found by plotting the pressure drop from tap 1 to each of the other taps against distance along the straight pipe (figure 12). A line representing $\frac{\Delta P}{\Delta L}$ was drawn through points 3 and 4 and extrapolated up to the beginning of the bend. Similarly, a line with the same slope was put through the point representing ΔP_{16} and extrapolated back to the bend. The vertical distance between these two lines represents ΔP_b. ΔP_s was found by subtracting $\frac{\Delta P}{\Delta L}$ times the length of the bend (if it were straightened out) from ΔP_b.

The line representing the frictional pressure loss $\left(\frac{\Delta P}{\Delta L}\right)$ was constructed through P_{16} because it was felt far enough away from the bend to be free of the turbulent effect of the bend. It was later shown by introducing a very fine stream of air bubbles into the water flow that the flow exhibits an oscillatory, rotational motion after it leaves the bend and that this motion damps out before it reaches the last pressure tap.

Figure 13 shows ΔP_b for all three bends plotted against Reynolds number on logarithmic paper. The plot is, in each case, a straight line with slope of 2, verifying the theory that ΔP_b is a function of R_e^2 (or V^2). The same results were found for ΔP_s for two of the bends but the values of secondary bend losses for the bend with R/D equal to 6 were so low that they were impossible to measure. The extrapolations of these curves were later used to determine the values of ΔP_b and ΔP_s

for water flows so low that the pressure drops could not be accurately measured.

4.22 Tests Performed With Two-Phase Flow

In order to determine the reliability of the apparatus in two-phase flow an attempt was made to verify the Martinelli correlation which has been previously discussed. $\left(\frac{\Delta P}{\Delta L}\right)_{TP}$ may be determined by using the methods of figure 12 if it is assumed that the two-phase flow is incompressible. This assumption will be valid if the pressure in the pipe and the flow quality are kept fairly low. Since the maximum quality investigated was less than .1 and the maximum pressure in the entry section was 10 psig the flow may be deemed incompressible.

It is important to realize that Martinelli compared the two-phase pressure drop to the pressure drop that would occur if water only were flowing with the same total mass rate of flow as the two-phase flow. In this investigation the ratio was calculated of the two-phase pressure drop to the pressure drop, that would occur if only the liquid phase were flowing, the gas phase not being present.

Equation 6 indicates that the pressure drop ratio is proportional to the flow rate raised to the 1.8 power. At a quality of .1, therefore, the experimental curve should differ from the Martinelli curve by the ratio of $\frac{W^{1.8}}{W^{1.8}(1-x)^{1.8}}$, or about 15%. At low qualities, however, there should be very

little difference between these two parameters since the total two-phase mass flow is almost equal to the mass flow rate of the water phase along.

In figure 14 the ratio of $\left(\frac{\Delta P}{\Delta L}\right)_{TP}$ to $\left(\frac{\Delta P}{\Delta L}\right)_{W}$ is plotted against quality. The experimental points are seen to be in good agreement with the Martinelli curve.

4.3 Range and Accuracy of Measured Results

The most severe restriction on the range of qualities that may be obtained is due to the fact that the maximum air flow is limited to one that will produce a pressure drop of 60 inches of water across the air nozzle. Any greater flow will tend to overflow manometer #2. Once the maximum air flow has been established through the system the greatest quality that may be obtained depends upon how small a water flow may be achieved. In order to measure these low flows a manometer filled with water (#4) was used rather than the regular mercury manometer to measure ΔH_w. The smallest flow that could be measured was about .3 pounds per second for below this flow even manometer number 4 became difficult to read. Since the air flow necessary for full scale manometer deflection was about .035 pounds/second the maximum possible quality was about .1.

It was not possible to measure friction and bend pressure drops for water flows for which manometer #4 was used.

The pressure drop between taps was only of the order of one or two tenths of an inch of mercury and this is about the limit to which the height of a column of mercury with its pronounced meniscus can be read. The frictional pressure drop, however, may be calculated by locating the friction factor in figure 11 and using equation 9. The bend and secondary losses can be found by using the extrapolated portions of the lines of figure 13.

A periodic pulsation or pressure surge was noticed in the two-phase flow which tended to make both the water-nozzle manometer fluid and the pressure-loss manometer fluid fluctuate about plus or minus .2 inches of mercury. The frequency of these surges seemed to decrease as the mass rate of water flow increased, as is shown in table II, and was the same in all cases for the pulsation of the mercury columns and the vibration of the apparatus itself. Since both the water-line and air-line pressures remained constant during each run it is believed that the vibrations arose in the mixer and were a result of injecting the air stream into the center of the stream of water.

Another source of error in measuring pressure drops in two-phase flow is the possibility of air being present in water-filled manometer lines. Although the lines were flushed with water between runs it was not possible to keep out all air at high mass flow rates. Since the pressure drop between taps 1 and 6 was between 15 and 20 inches of mercury for these flows

and most of the air that was ever forced into the lines was between 2 and 3 inches of water (about .2 in. Hg.) the error in measuring the pressure drop amounted to only 1%.

V RESULTS

The results of this investigation are presented in Table III and Figures 14 to 20. Figure 14 represents an attempt to verify the Martinelli correlation in order to establish the repeatibility and realiability of the test apparatus. Agreement of the data with the Martinelli curve is seen to be good with most of the scatter of points appearing quite random. It is expected, however, that if the range of qualities investigated was extended much beyond .1 the experimentally derived curve would tend to fall below that of Martinelli because of the difference in defining $\left(\frac{\Delta P/\Delta L}{\Delta P/\Delta L}\right)_{w}^{tp}$ (Sect. 2.1).

Figures 15 through 17 represent plots of the ratio of two-phase total bend pressure drop to that for water as a function of the flow quality for each of the three bends, Since both the two-phase and the water pressure drops were large and accurately read for the bend with relative radius equal to 1 and this bend gives a curve with very little scatter it is believed that a great deal of the scatter of experimental points in the other two figures is due to the inaccuracy of measuring the lower pressure drops for these other bends. In addition to representing the experimental points the curves must pass through a pressure ratio of 1 at zero quality since at this quality the two-phase flow degenerates into a flow of water only. For reasons of clarity of presentation

this additional point was not shown on these curves.

The curves of Figures 15, 16 and 17 are compared in figure 18. Although these results do not completely agree with those predicted in Section III, they are significant in showing that the Martinelli correlation does not adequately predict the two-phase pressure drop in a pipe bend. At a quality of .1 the ratio of two-phase pressure drop to single-phase pressure drop for bends with R/D equal to 1 and 6 is 25% greater than that predicted by Martinelli. Although insufficient data was obtained for a relative radius of 4 to accurately draw a curve it is seen that the data plotted lies well below that of Martinelli. The same phenomenon, it will be seen, occurs if secondary rather than total bend losses are plotted, as in Figure 19.

The author was unable to add a curve representing a relative radius of 6 to figure 19 because, as was discussed, the secondary losses in water flow were small and difficult to measure. The form and the relative position of the two curves in figure 19, however, agree with the predictions of Castillo (figure 21) although his relative secondary pressure losses are lower in magnitude by about half than those actually measured.

Beij's results with water show that the ratio of total to frictional pressure loss in a bend is a function only of R/D. Applying this to two-phase flow yielded the curves of figure 20, establishing $\frac{\Delta P_{\phi}}{\Delta P_{F}}$ as a parameter in two-phase

as well as in liquid flow. According to these results two-phase flow through a sharp bend will yield a higher bend loss relative to the friction loss than will a water flow through the same bend. For milder bends the relative bend loss approaches that for water and for an R/D of infinity (i. e., a straight pipe) they both approach a value of 1. Since a flow of water and air may be considered to have a very large density ratio and a flow of water be considered a two-phase flow with a density and viscosity ratio of 1 a flow of a mixture of any liquid and gas may be expected to lie between the two curves plotted in Figure 20.

A great deal of data was taken for the special case of stratified flow. Although this data is not included in this report, it was used by Castillo in an inquiry into the nature of stratified flow. It is Castillo's belief that a great deal of the pressure loss in a separated flow around a bend arises from rotation of the liquid in the bend. He has used this data to verify his analytical results and they will soon be published in an M.I.T. S.M. Thesis (4).

When an annular flow which was just on the verge of becoming separated was investigated it was found that the separation did occur in the bend, the flow remaining separated throughout the remainder of the exit section. These results are again in accordance with Castillo's theory that a part of the bend secondary loss is due to the tendency of the flows to separate.

VI CONCLUSIONS AND RECOMMENDATIONS

6.1 Conclusions

As a result of this investigation the following is concluded:

(1) The ratios of the total two-phase pressure loss in a bend and the two-phase pressure loss due to factors other than friction to the total bend pressure loss in a flow of water and the secondary bend pressure loss for water, respectively, are functions only of the quality of the flow and the relative radius of the bend. The relationship tends to take the form of Eq. 7, the Martinelli correlation of two-phase pressure drop in straight pipes. The form of the curves, when plotted, agrees with the predictions of Castillo although the pressure ratios are greater in magnitude than those at which he has arrived.

(2) Martinelli's correlation with quality of the ratio of two-phase straight pipe pressure drop to that of a single phase does not adequately describe the pressure loss in a pipe bend. The actual pressure drop ratio may either be higher or lower than that predicted by Martinelli. For relative bend radii of 1 and 6 it was found to be 25% higher at a quality of .1 and at the same quality the ratio for a bend with R/D of 4 was lower by the same amount.

(3) As is the case in liquid flow the ratio of the total pressure drop across a bend to the pressure drop due only to friction appears to be a function only of R/D also in two-phase flow. For very sharp bends this ratio is a great

deal higher for two-phase flow than it is for water flow.

6.2 Recommendations

The author sincerely hopes that future work along these lines will be accomplished. It is his contention, however, that the apparatus be slightly modified if the investigation is to be continued.

A fair amount of inaccuracy was imparted to the data by the turbulence and unsteadiness of the flow caused by the jet-type mixer. It is suggested that this mixer be replaced by one of more reliable performance and of perhaps simpler operation. A simple "Y"-type pipe connection will most probably be quite sufficient. If stratified flow is desired, a flat piece of metal may be placed horizontally in the middle of the outlet of the "Y", to initiate a separated flow. Such a mixer has been used with success by Strawson (6) in his investigation of velocity profile in stratified flow in a rectangular conduit.

In order to more accurately measure small bend pressure drops it is suggested that the sensitivity of the manometer system be increased. At the same time it is felt that using a heavier fluid in the air-nozzle manometer or changing the nozzle design will allow a greater air flow and the investigation of a greater range of qualities.

Data for two-phase secondary pressure drop for R/D of 6 is included in this report (Table III) so if the data

for water only could be obtained the curve missing from Figure 19 could be drawn. It would be interesting to see whether or not this curve will agree with Castillo's predictions.

Data should be obtained for bends with relative radii other than those considered in this investigation. Since the pressure drop characteristics of bends with R/D equal to 1 and 4 are so different it is suggested that R/D of 2 and 3 be carefully investigated.

APPENDIX I

INSTRUMENTATION

1. Flow Nozzles

A.S.M.E. Long-Radius, High Ratio nozzles were installed in both the air and the water lines in order to measure the flow of the fluids before mixing. The design of the water nozzle used is shown in figure (7). The air nozzle is geometrically similar, all its dimensions being twice those of the water nozzle. In the case of the water flow the pressure drop across the nozzle, ΔH_w, was measured by a U-tube mercury filled manometer (number 1, figure 4) and the A.S.M.E. formulas were used to calculate the mass rate of flow, W_w. The nozzle coefficient, K, was read from figure 2 and substituted into:

$$w_w = .668 A_2 K Y \sqrt{\rho \Delta P} \qquad \text{(Eq.A 1) (8)}$$

where:

w_w = mass rate of flow of water,

A_2 = throat area of the nozzle

Y = a valve of 1 for incompressible fluids

P = density of water

ΔP = pressure drop across the nozzle.

Figure 8, a plot of W_w against ΔP_w, shows the results of calculations based upon eq. A 1.

At low flow rates, ΔH_w less than 3 in. Hg., it was not possible to obtain an accurate reading of the mercury

manometer so manometer number 4, using a column of water rather than mercury, was used. The low flow rates corresponding to various manometer readings were measured by a weigh tank and the curve of Figure 9 drawn.

For the air flow the A.S.M.E. formulas were again used with the later substantiated assumption that the pressure drop across the air nozzle is less than 10% of the pressure in the air stream as it enters the nozzle. For such a case

$$w_a = .1615\, c\, D_2^2 \frac{\sqrt{\rho \Delta P / T}}{\sqrt{1 - \left(\frac{D_2}{D_1}\right)^4}} \qquad \text{(A 2)}$$

where

- c = .99 for all the air flows investigated
- D_2 = nozzle throat diameter
- D_1 = nozzle inlet diameter
- T = absolute temperature of air stream
- ρ = absolute pressure of air stream
- ΔP = pressure drop across the nozzle.

The pressure drop across the nozzle, ΔH_a, was measured in inches of water by a U-tube manometer (#2). For air flows of less than 5 inches of water a micromanometer was used.

2. Pressure Drop Measurement

A reservior-type manometer (#3) was employed to measure, in inches of mercury, the pressure drop between the first pressure tap and any of the others. To the top of this manometer was attached a can which was connected by valves to

the manometer lines and kept full of water. If any air bubbles should become trapped in a line the valve was opened allowing water from the can to flush the line.

In filling the reservoir manometer too much mercury was used and it overflowed from the reservoir into the thin inlet tube which connects it to the pressure tap. Since the scale of this type of manometer is calibrated to take into consideration only the relatively small change in height of the liquid in the large reservoir any mercury in the narrow connecting tube will lead to an erroneous pressure measurement. Much of the data had been taken before this error was noticed so it was decided to calibrate the manometer rather than retake the data. By attaching a regular U-tube manometer to the reservoir manometer the calibration curve of figure 10 was obtained. Since the dotted line represents the case of the two manometers being in complete agreement it is seen that at a pressure drop of 7.3 inches of mercury the reading of the reservoir manometer becomes the true pressure drop. This is to be expected since at this point the mercury level has dropped back into the reservoir and the erroneous effect of the narrow tube is no longer present.

APPENDIX II - TABULATED RESULTS

Table 1 - Results With Water Flow

W_w	$R_e \times 10^{-4}$	f	$\Delta P/\Delta L$	ΔP_b R/D = 6	ΔP_b R/D = 4	ΔP_s R/D = 4	ΔP_b R/D = 1	ΔP_s R/D = 1
0.641	2.09	.0310	.0063	.05	----	----	0.09	0.083
0.840	2.74	.0300	.0104	.10	0.17	.117	0.14	0.127
1.200	3.91	.0280	10196	.15	0.39	.303	0.38	0.300
1.488	4.85	.0281	.0304	.24	0.51	.370	0.44	0.403
1.725	5.63	.0262	.0384	.28	0.59	.405	0.63	0.585
1.937	6.31	.0229	.0424	.45	----	----	----	------
2.130	6.95	.0223	.0528	.620	0.55	.260	----	------
2.465	8.05	.0215	.0649	.78	1.16	.860	----	------
2.622	8.55	.0220	.0752	.85	----	----	----	------
2.770	9005	.0248	.0960	---	----	----	1.42	1.310

Table 2 - Frequency Of Two-Phase Pressure Pulsations

W_w	W_a	x	fluctuations --minute--
.277	.0122	.042	77
.485	.0077	.015	80
.445	.0122	.027	81
.445	.0173	.038	97
.420	.0040	.010	176
.400	.0021	1005	180
.270	.0292	.098	320
.225	.0335	.129	350
1260	.0345	.117	384

Table 3 - Results With Two - Phase Flow

W_w	$W_a \times 10^{-3}$	X (10^{-3})	$\frac{\Delta P}{\Delta L}$	ΔP_b	ΔP_s	$\left(\frac{\Delta P_{TP}}{\Delta P_w}\right)_f$	$\left(\frac{\Delta P_{TP}}{\Delta P_B}\right)_B$	$\left(\frac{\Delta P_{TP}}{\Delta P_w}\right)_S$
R/D = 6								
0.641	7.8	12.0	.044	0.96	0.65	7.6	19.2	----
	10.9	16.7	.064	0.78	0.33	10.2	15.6	----
	14.1	21.5	.065	1.24	0.78	10.3	24.8	----
	16.9	25.7	.098	0.95	0.26	10.5	19.0	----
	20.5	30.8	.117	0.95	0.12	18.6	19.0	----
	23.5	35.7	.128	1.03	0.13	20.4	20.6	----
	26.3	39.8	.150	1.25	0.19	23.9	25.0	----
	30.8	46.0	1178	1.03	----	28.3	20.6	----

Table 3 -- Continued

W_w	Wa X 10^{-3}	x (10^{-3})	$\frac{\Delta P}{\Delta L}$	ΔP_b	ΔP_s	$\left(\frac{\Delta P_{TP}}{\Delta P_w}\right)_F$	$\left(\frac{\Delta P_{TP}}{\Delta P_w}\right)_B$	$\left(\frac{\Delta P_{TP}}{\Delta P_w}\right)_S$
R/D = 6								
0.840	8.1	9.5	.068	1.47	1.07	6.5	14.7	----
	11.2	13.2	.076	1.98	1.44	7.3	19.8	----
	12.7	14.8	.096	1.50	.820	9.2	15.0	----
	15.0	17.5	.120	1.72	0.87	11.5	17.2	----
	17.8	20.7	.108	2.35	1.59	10.4	23.5	----
	21.4	24.9	.116	2.81	1.95	11.2	28.1	----
	24.7	28.6	.124	3.42	2.54	11.9	34.2	----
	29.6	34.0	.152	3.25	2.68	14.6	32.5	----
1.200	8.1	6.7	.086	1.75	1.14	4.4	11.7	----
	11.8	9.8	.106	2.67	1.92	5.9	17.8	----
	12.9	10.6	.126	2.30	1.41	6.4	15.3	----
	15.4	12.7	.138	3.28	2.30	7.1	21.8	----
	18.0	14.8	.151	3.59	2.53	7.7	23.9	----
	22.1	18.1	1184	3.69	2.39	9.4	24.6	----
	25.3	20.6	.216	4.52	3.00	11.0	30.1	----
	28.3	23.0	.244	4.45	2.73	12.45	29.7	----
	31.0	25.2	.248	4.65	2.90	12.65	31.0	----
	33.2	26.9	.284	4.39	2.39	14.5	29.3	----
	36.0	29.1	.239	5.96	4.27	12.2	3917	----
1.488	8.2	5.5	.128	1.53	.62	4.2	6.4	
	11.8	7.8	.144	1.93	1.93	4.7	12.3	----
	13.0	8.7	.184	2.19	.89	6.1	9.2	----
	15.2	10.1	.200	3.10	1.69	6.6	12.9	----
	18.2	12.1	.232	2.84	1.20	7.5	11.8	----
	22.1	14.6	.256	3.86	2.06	8.4	16.1	----
	25.0	16.5	.256	4.16	2.36	8.4	17.3	----
	28.3	18.7	.256	5.66	3.66	8.4	22.7	----
	31.0	20.4	.248	6.75	5.00	8.2	28.1	----
	35.5	23.3	.256	7.46	5.60	8.4	31.1	----
1.725	8.2	4.7	.124	1.72	.84	3.2	6.2	----
	12.0	6.9	.172	2.98	1.76	4.5	10.7	----
	13.0	7.5	.188	3.79	2.46	4.9	13.5	----
	15.4	8.9	.184	4.59	3.29	4.8	16.4	----
	18.5	10.6	.200	5.00	3.49	5.2	17.85	----
	22.1	12.7	.260	5.23	3.41	6.7	18.8	----
	25.0	14.3	.264	5.97	4.10	6.9	21.4	----
	28.3	16.0	.280	6.29	4.31	7.3	22.5	----
	31.0	17.7	.280	7.29	5.31	7.3	26.0	----

Table 3 - Continued

W_w	W_a	$X \times 10^{-3}$	$x_{(10^{-3})}$	$\frac{\Delta P}{\Delta L}$	ΔP_b	ΔP_s	$\left(\frac{\Delta P_{TP}}{\Delta P_w}\right)_F$	$\left(\frac{\Delta P_{TP}}{\Delta P_w}\right)_B$	$\left(\frac{\Delta P_{TP}}{\Delta P_w}\right)_s$
R/D = 6									
0.260	23.9	84.1	.064	0.60	0.150	53.5	----	----	
0.265	17.2	62.0	.030	1.05	0.830	24.5	99.9	----	
0.270	7.8	28.0	.024	0.11	-----	18.9	11.0	----	
0.270	29.2	97.7	.076	0.72	0.190	58.4	72.0	----	
0.277	12.2	42.1	.045	0.26	-----	33.3	26.0	----	
0.325	23.9	68.5	.063	1.13	0.690	34.8	84.0	----	
0.406	29.0	66.7	.075	1.40	0.880	28.8	67.0	----	
0.413	23.6	54.0	.075	1.10	0.580	27.3	----	----	
0.445	17.3	37.5	.053	1.36	0.990	16.6	55.6	----	
0.445	12.2	26.7	.052	1.20	0.830	16.2	49.0	----	
0.485	7.7	15.6	.054	0.44	0.050	14.4	15.2	----	
0.382	19.7	49.0	.0072	0.82	0.310	29.4	44.3	----	
0.375	12.0	31.9	.032	1.13	0.900	13.5	62.80	----	
0.368	25.2	65.3	.076	0.93	0.420	33.2	54.7	----	
0.317	23.7	75.0	.068	0.87	0.390	46.0	79.0	----	
0.292	23.7	75.0	.068	0.87	0.390	46.0	79.0	----	
R/D = 4									
0.840	17.4	20.3	.140	2.00	1.340	12.5	11.8	11.5	
	21.4	24.9	.170	1.97	1.110	15.2	11.6	9.5	
	24.4	28.3	.188	1.97	1.080	16.8	11.6	9.2	
	28.3	34.0	.206	2.26	1.290	18.4	13.3	11.0	
	34.0	39.0	.220	3.32	2.280	19.7	19.5	19.5	
1.200	17.4	14.3	.183	2.97	2.110	10.0	7.6	7.0	
	24.4	19.9	.220	4.02	3.000	12.0	10.4	9.9	
	29.6	24.0	.294	4.05	2.670	16.0	10.5	8.8	
	34.0	27.5	.318	4.27	2.780	17.3	11.0	9.2	
R/D = 1									
0.840	13.5	15.7	.130	0.90	0.747	11.8	6.4	5.9	
	18.7	21.8	.130	2.55	2.397	11.8	18.2	18.9	
	22.7	26.3	.152	2.85	2.670	13.80	20.4	21.0	
	25.8	29.8	1175	3.50	3.290	15.9	25.0	25.9	
	31.3	35.9	.184	5.29	5.070	16.7	37.8	40.0	
	35.8	40.8	.192	5.99	5.760	17.5	42.7	45.5	

Table 3 - Continued

W_w	W_a X 10^{-3}	x (10^{-3}) $\frac{\Delta P}{\Delta L}$	ΔP_b	ΔP_s	$\left(\frac{\Delta P_{TP}}{\Delta P_w}\right)_f$	$\left(\frac{\Delta P_{TP}}{\Delta P_w}\right)_B$	$\left(\frac{\Delta P_{TP}}{\Delta P_w}\right)_s$
R/D = 1							
1.200	13.5	11.1	.177	2.62	2.41	9.3	6.9	8.0
	18.7	15.4	.203	4.24	4.00	10.6	11.2	13.1
	22.7	18.6	.263	4.09	3.78	13.7	10.8	12.60
	25.8	21.1	.280	5.08	4.75	14.6	14.0	15.80
	31.3	25.5	.296	6.10	5.75	15.4	16.0	19.1
	35.8	29.0	.312	6.60	6.23	16.2	18.3	20.7
1.4800	13.5	9.1	.192	3.79	3.56	6.2	8.6	8.8
	18.7	12.5	.238	4.19	3.91	7.6	9.5	9.7
	22.7	15.1	.248	5.85	5.56	8.0	13.3	13.7
0.411	13.5	29.8	.065	1.28	1.20	22.6	32.8	33.7
0.361	18.3	48.5	.071	1.30	1.22	32.0	42.0	43.0
0.361	22.7	59.3	.061	2.18	2.11	27.5	70.0	74.4
0.300	25.8	79.0	.072	1.57	1.49	43.4	73.0	76.5
0.300	31.0	93.5	.081	1.73	1.63	48.7	80.5	83.5
0.260	18.3	66.0	.044	0.97	0.92	34.4	58.8	61.4

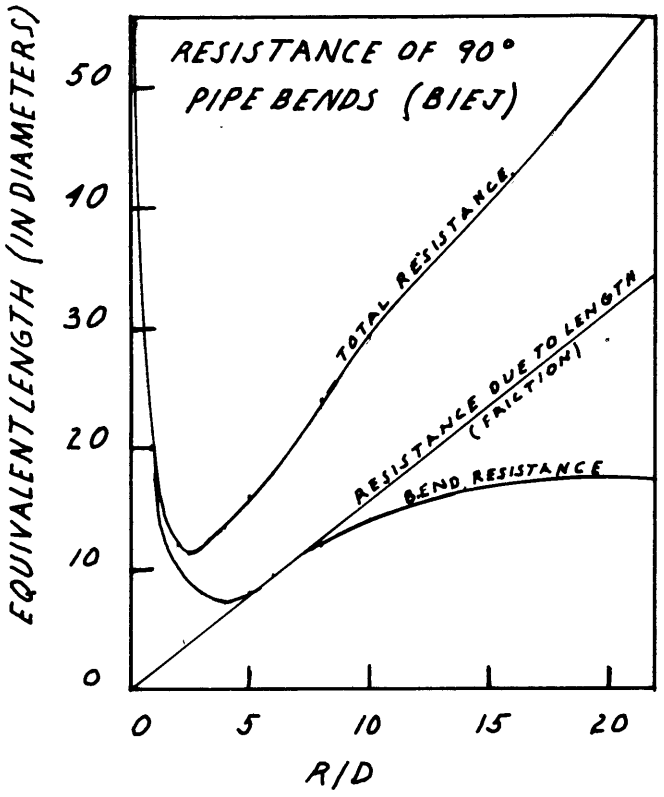

FIGURE 1

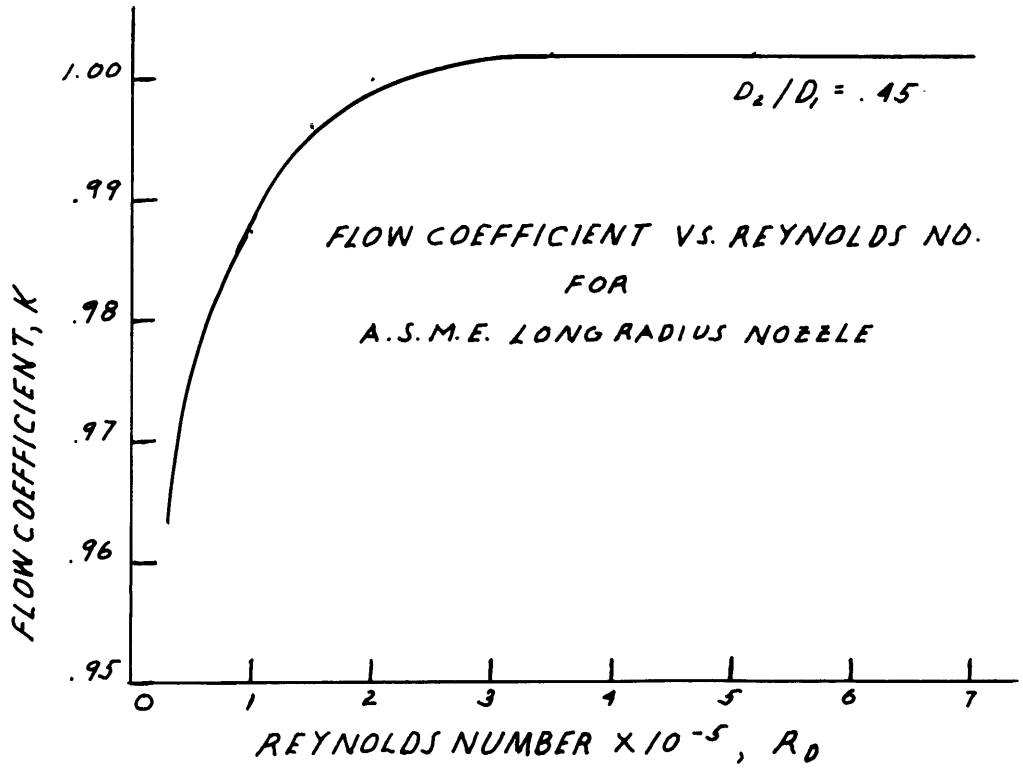

FIGURE 2

FIGURE 3

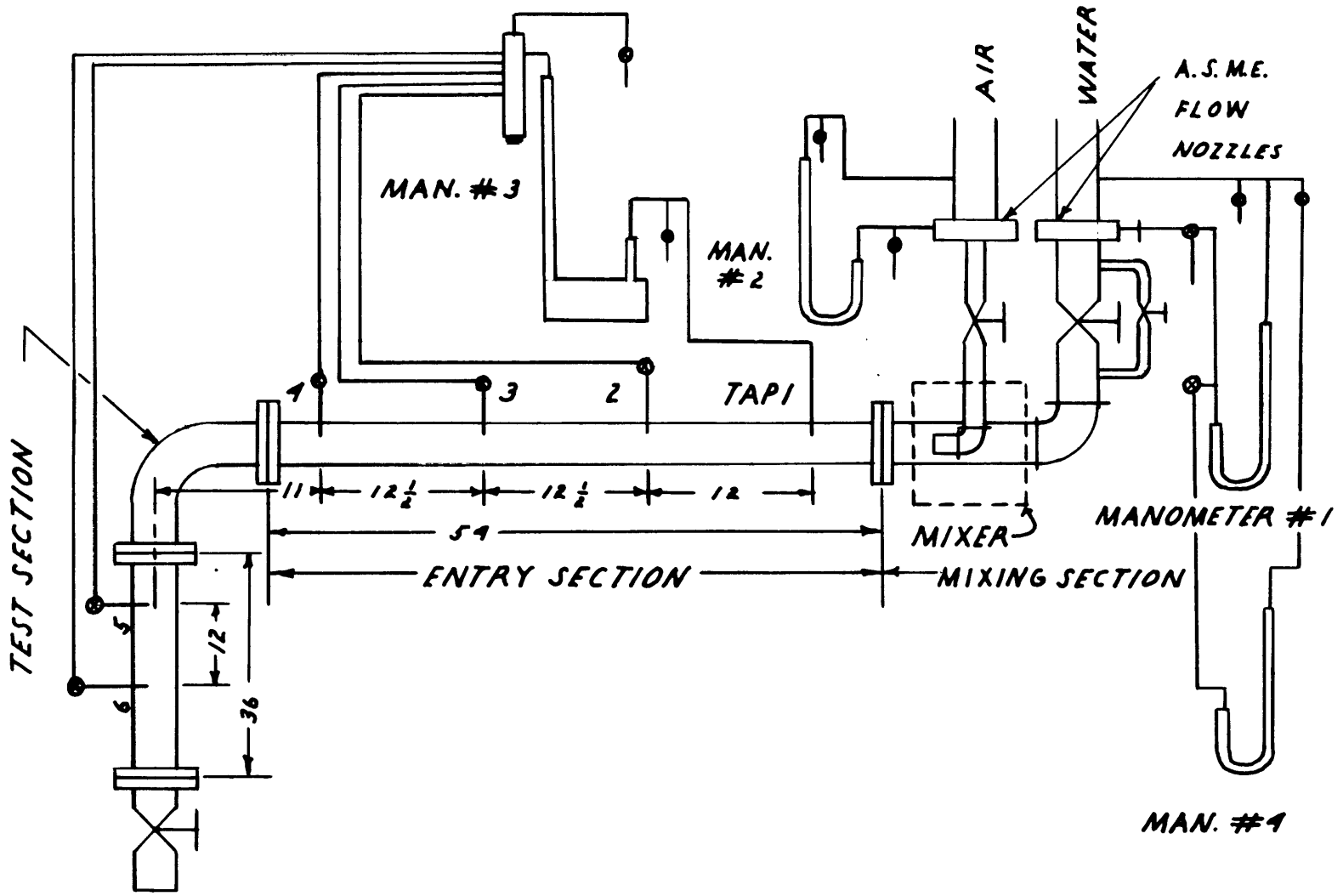

SCHEMATIC DIAGRAM OF APPARATUS

FIGURE 1

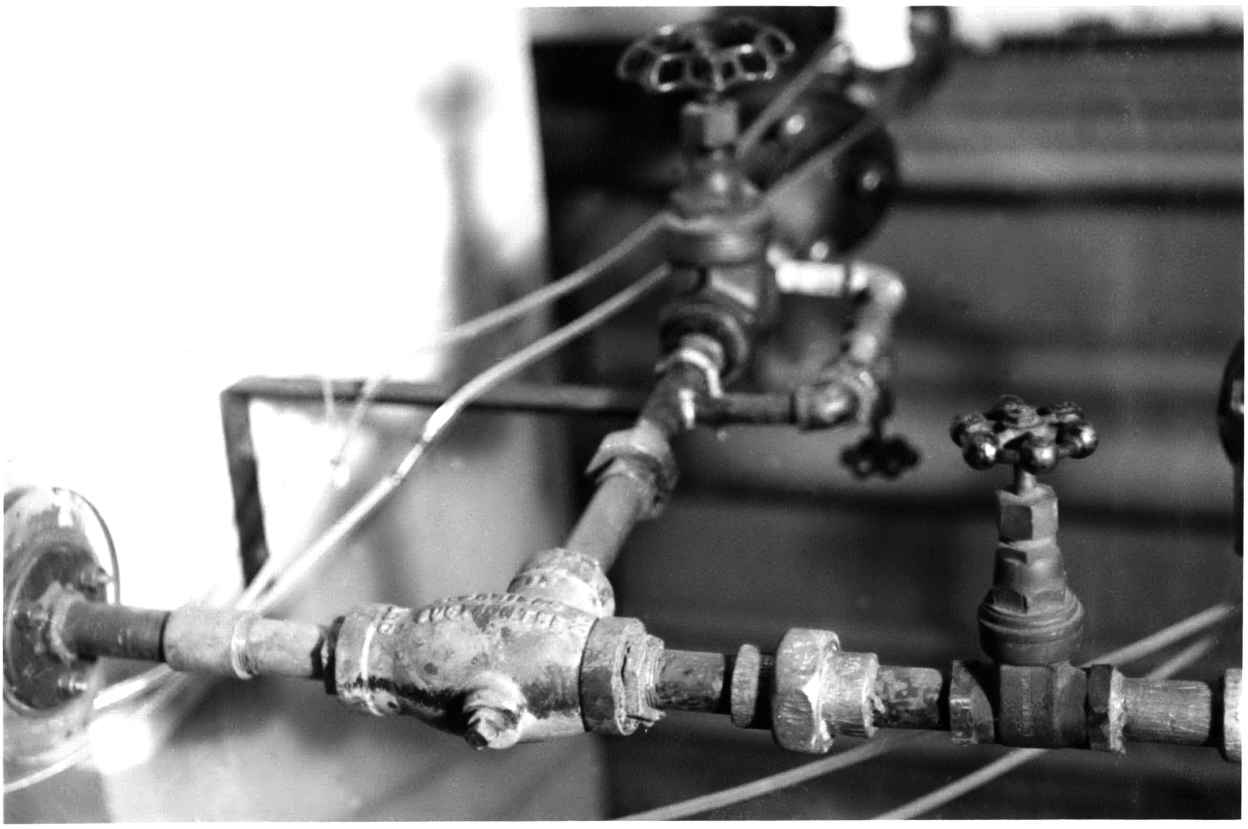

FIGURE5

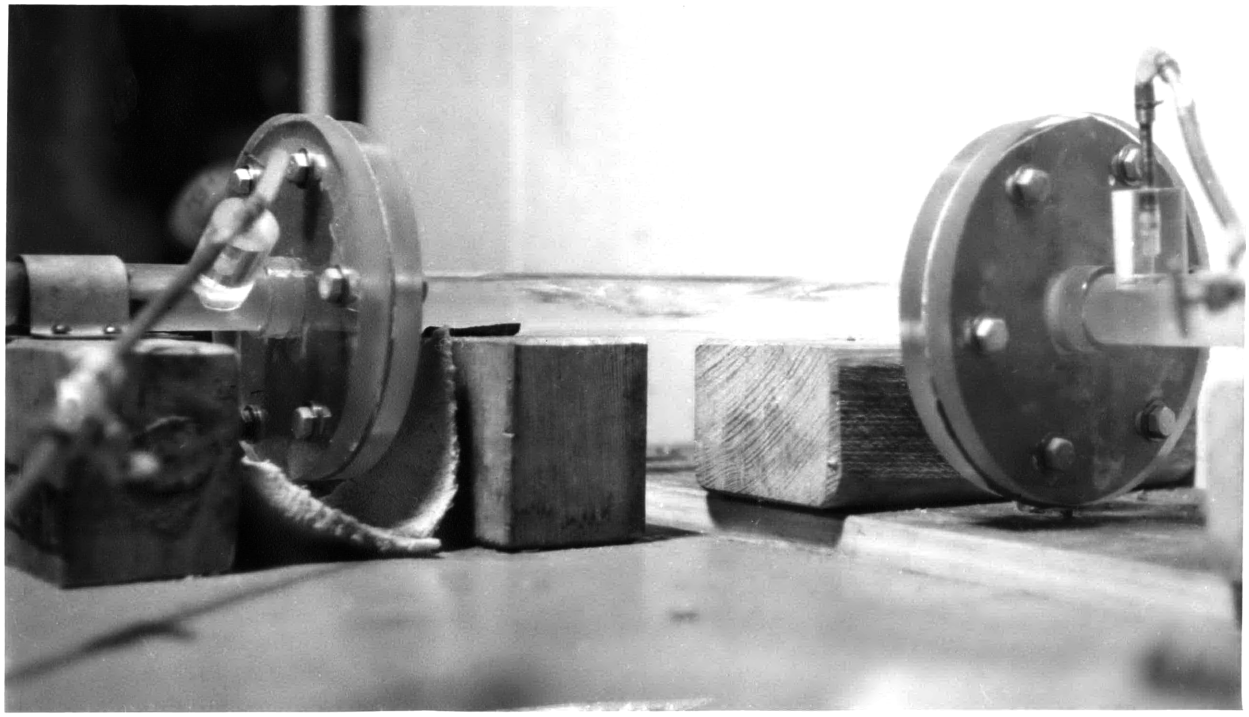

FIGUAE 6

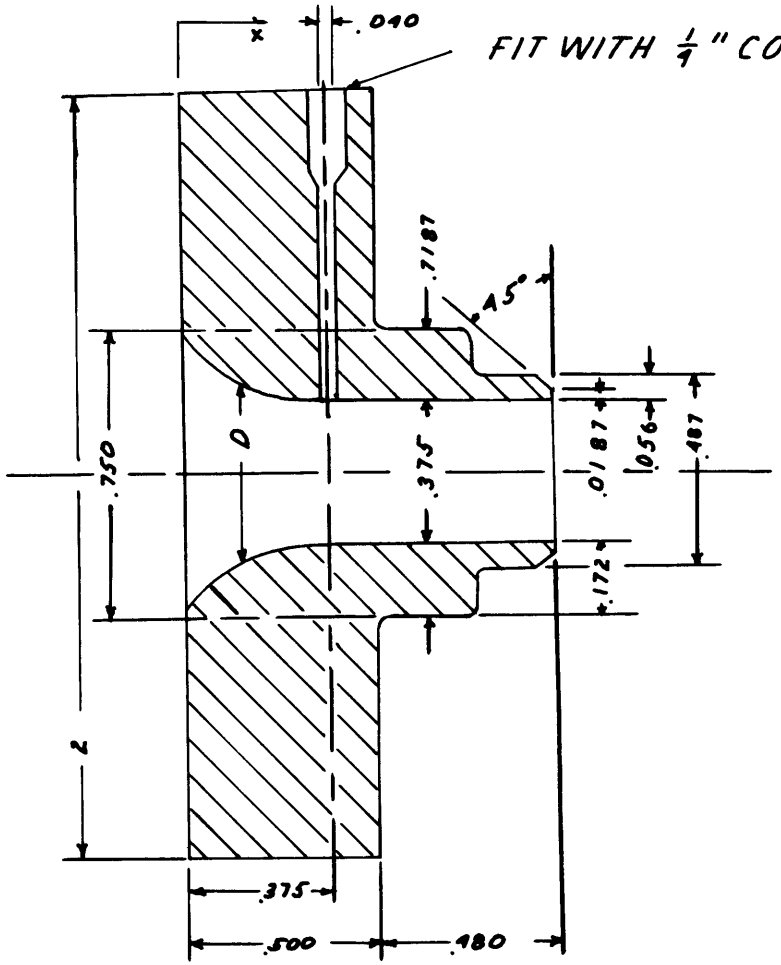

A.S.M.E. LONG-RADIUS HIGH-RATIO NOZZLE
NOZZLE NO. 1 ~ BRASS

FIGURE 7

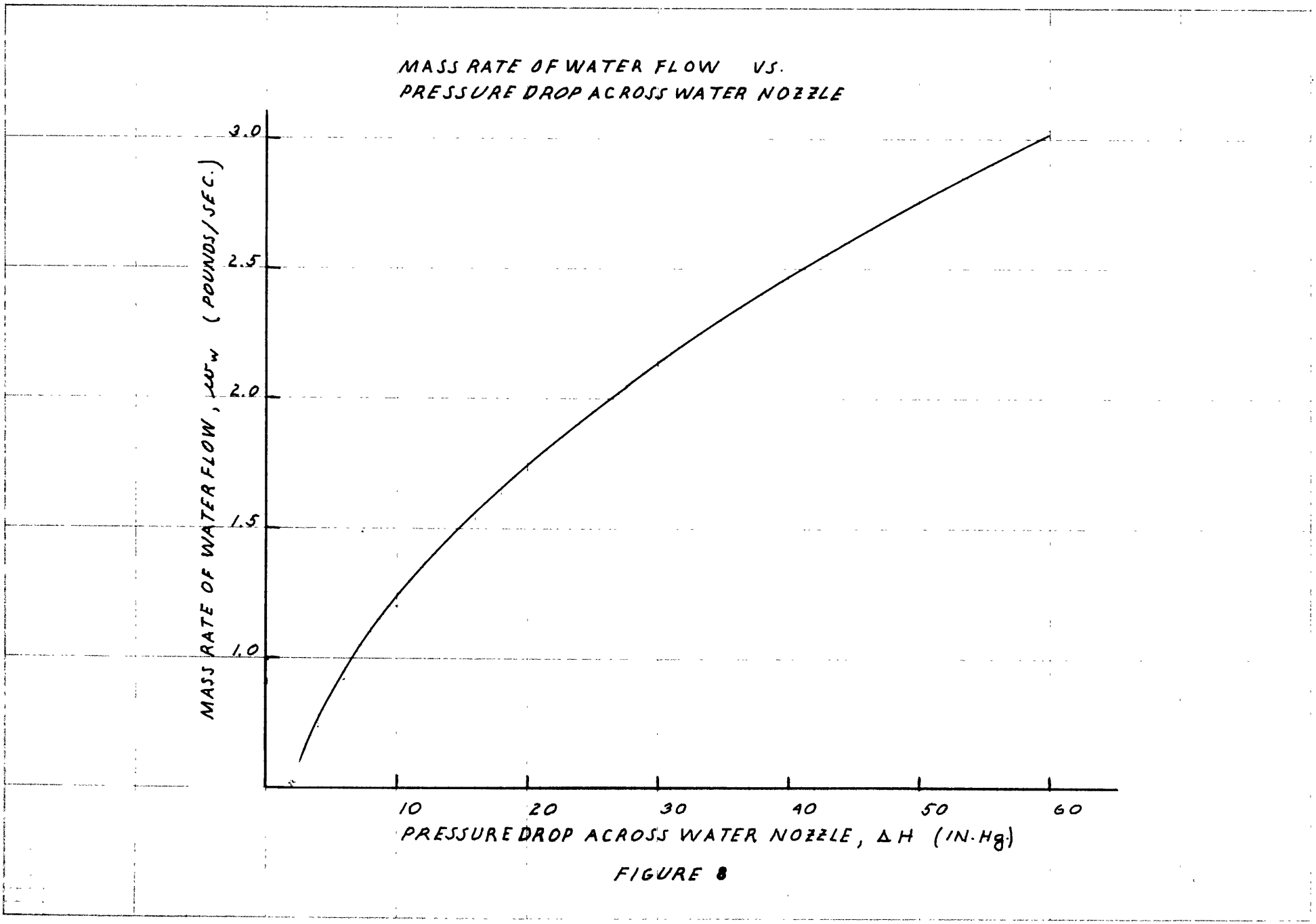
MASS RATE OF WATER FLOW VS.
PRESSURE DROP ACROSS WATER NOZZLE
MASS RATE OF WATER FLOW, w_w (POUNDS/SEC.)
3.0
2.5
2.0
1.5
1.0
10
20
30
40
50
60
PRESSURE DROP ACROSS WATER NOZZLE, ΔH (IN. Hg)

FIGURE 8

MASS RATE OF WATER FLOW VS.
PRESSURE DROP ACROSS WATER NOZZLE
(FOR LOW WATER FLOWS)

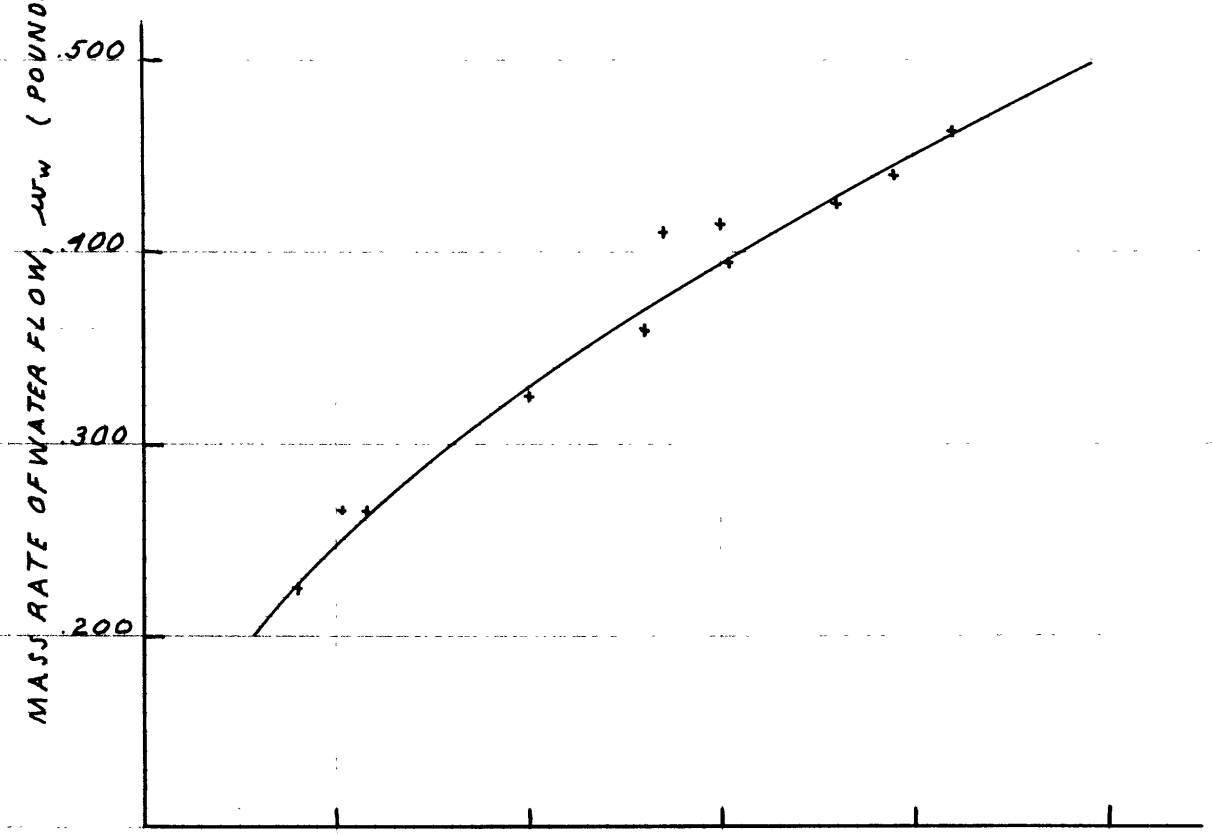

FIGURE 9

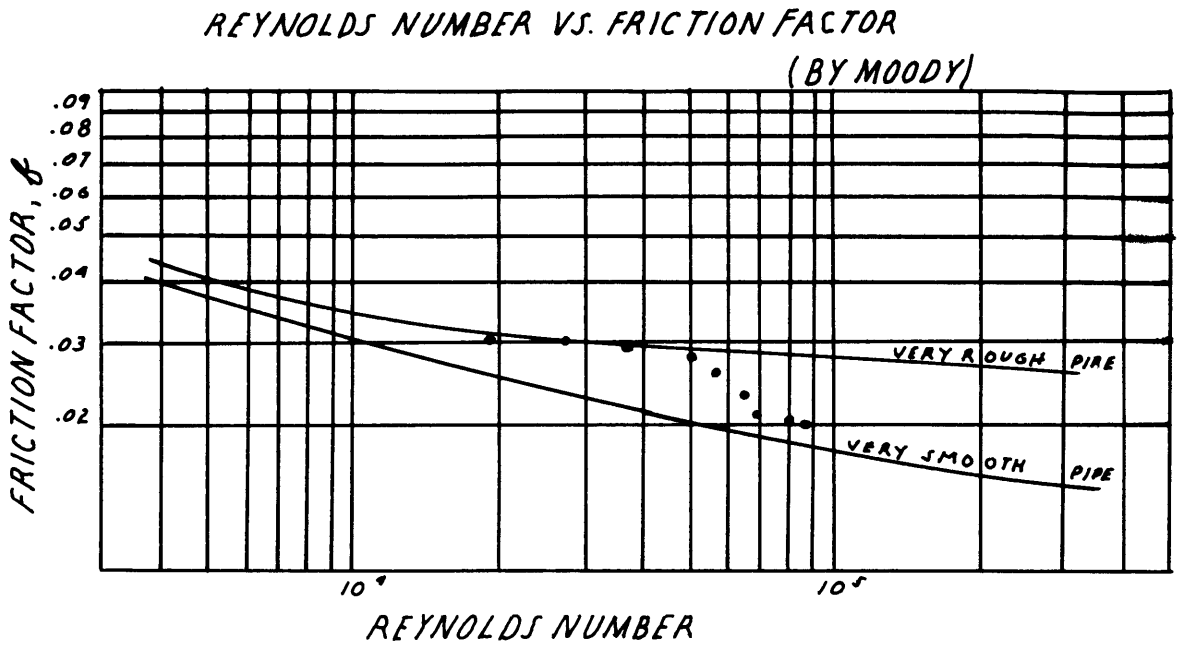

FIGURE 11

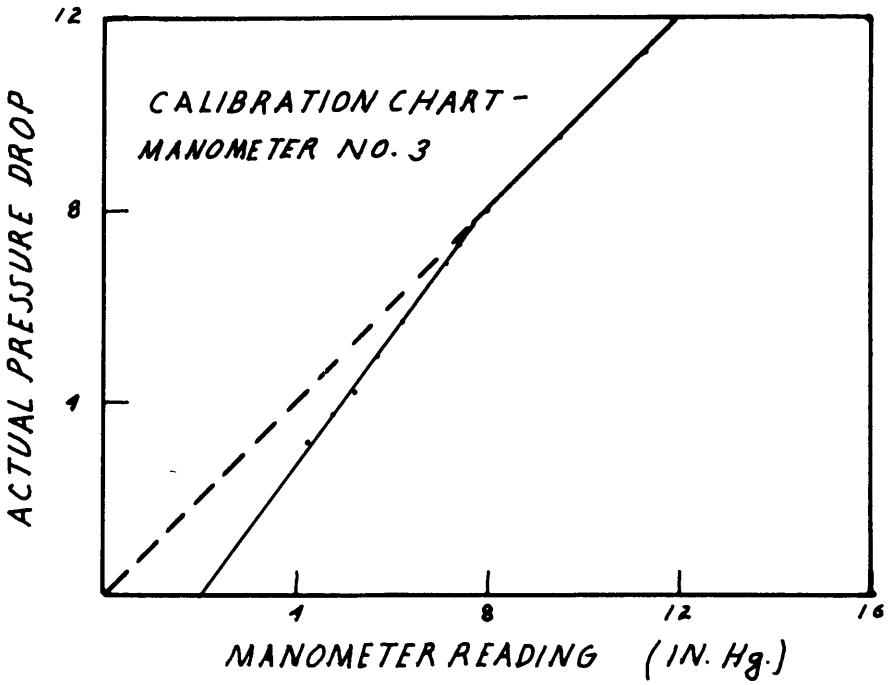

FIGURE 10

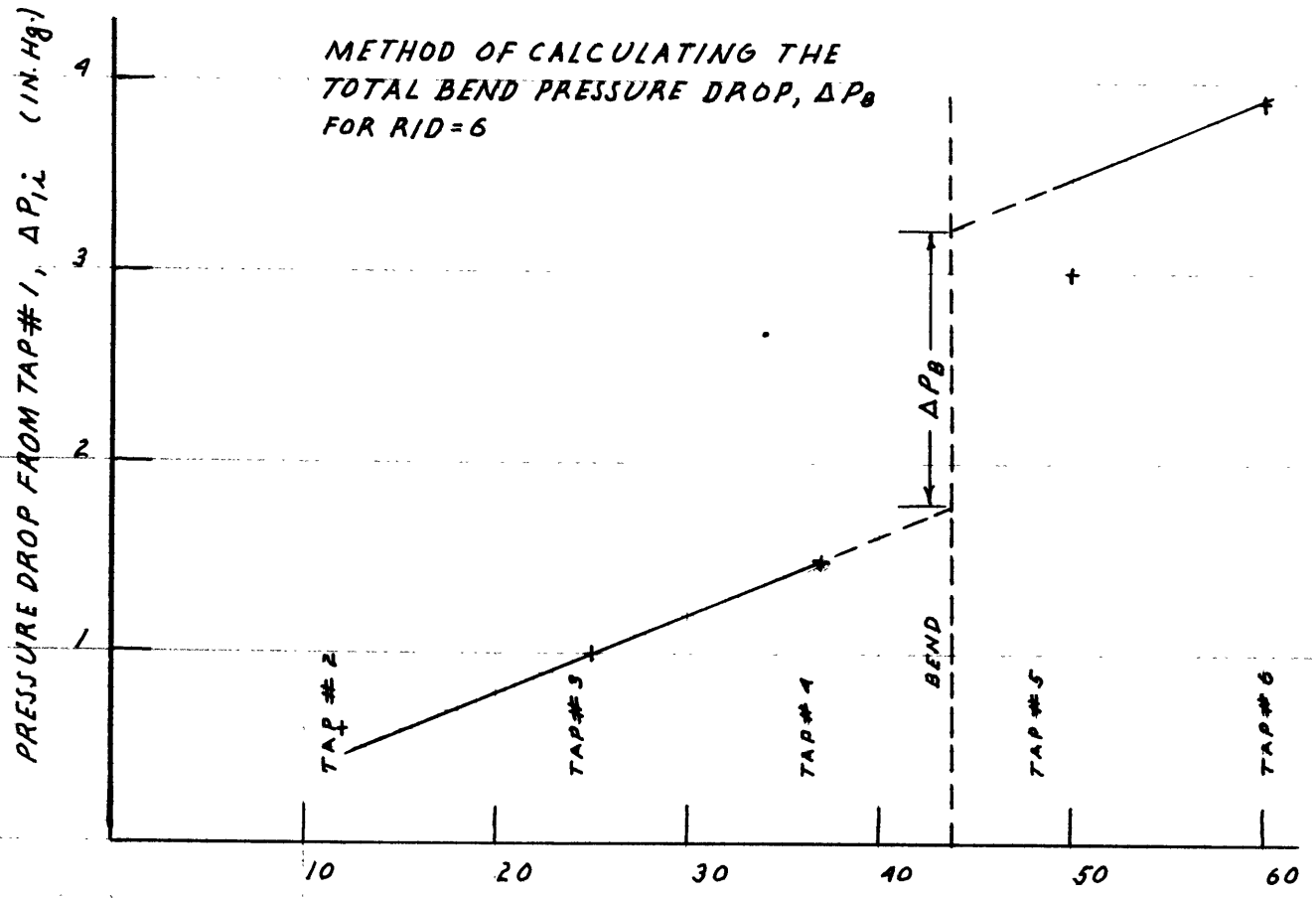
METHOD OF CALCULATING THE
TOTAL BEND PRESSURE DROP, ΔP_B
FOR R/D = 6
PRESSURE DROP FROM TAP #1, ΔP_1i (IN. Hg.)
4
3
2
1
ΔP_B
TAP #2
TAP #3
TAP #4
BEND
TAP #5
TAP #6
10
20
30
40
50
60
DISTANCE ALONG STRAIGHT PIPE

FIGURE 12

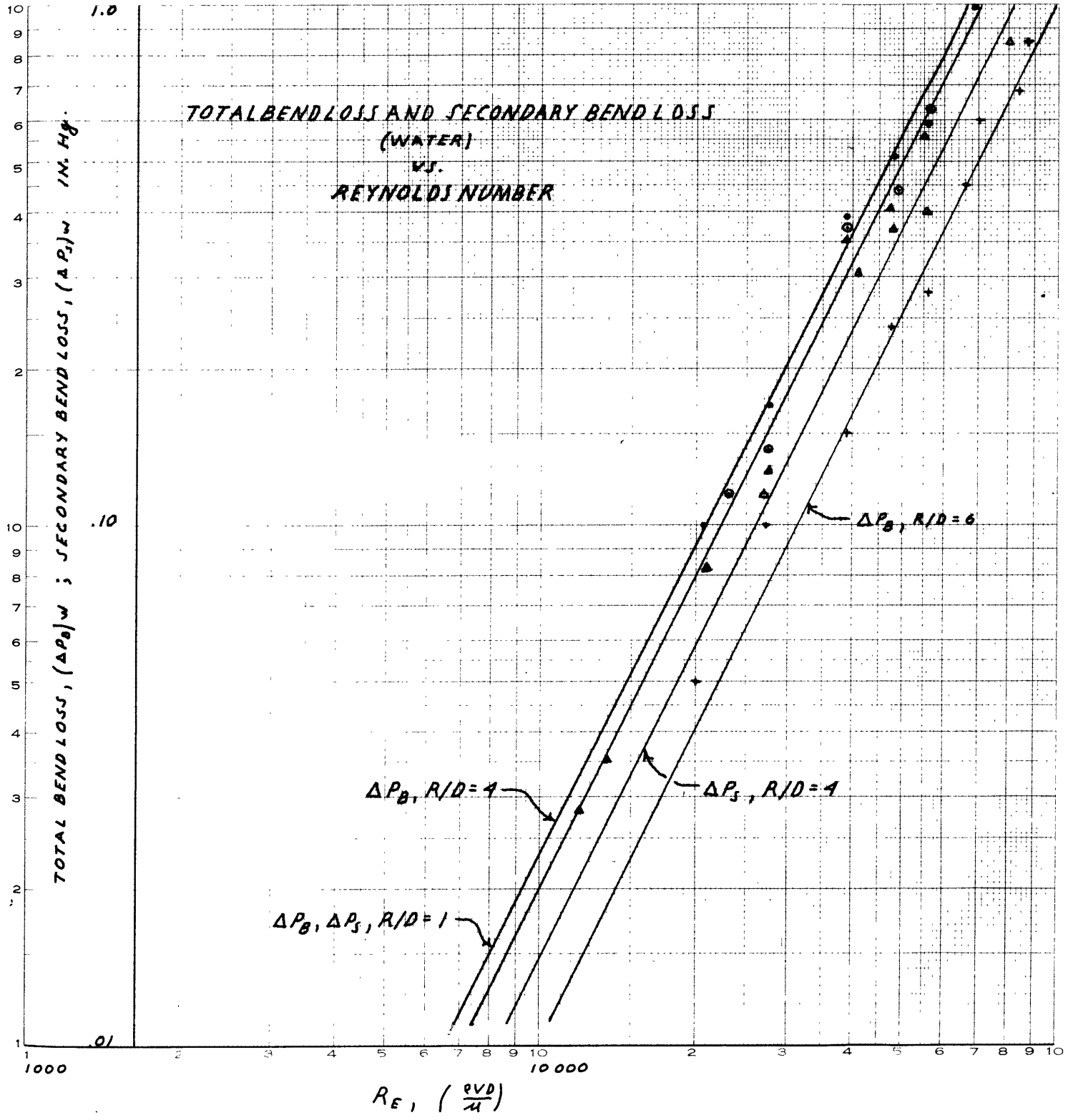
TOTAL BEND LOSS AND SECONDARY BEND LOSS
(WATER)
VS.
REYNOLDS NUMBER
TOTAL BEND LOSS, $(\Delta P_B)_W$; SECONDARY BEND LOSS, $(\Delta P_S)_W$ IN. Hg.
1.0
.10
.01
ΔP_B, R/D = 6
ΔP_B, R/D = 4
ΔP_S, R/D = 4
ΔP_B, ΔP_S, R/D = 1
1000
10 000
R_E, $\left(\frac{\rho V D}{\mu}\right)$

FIGURE 13

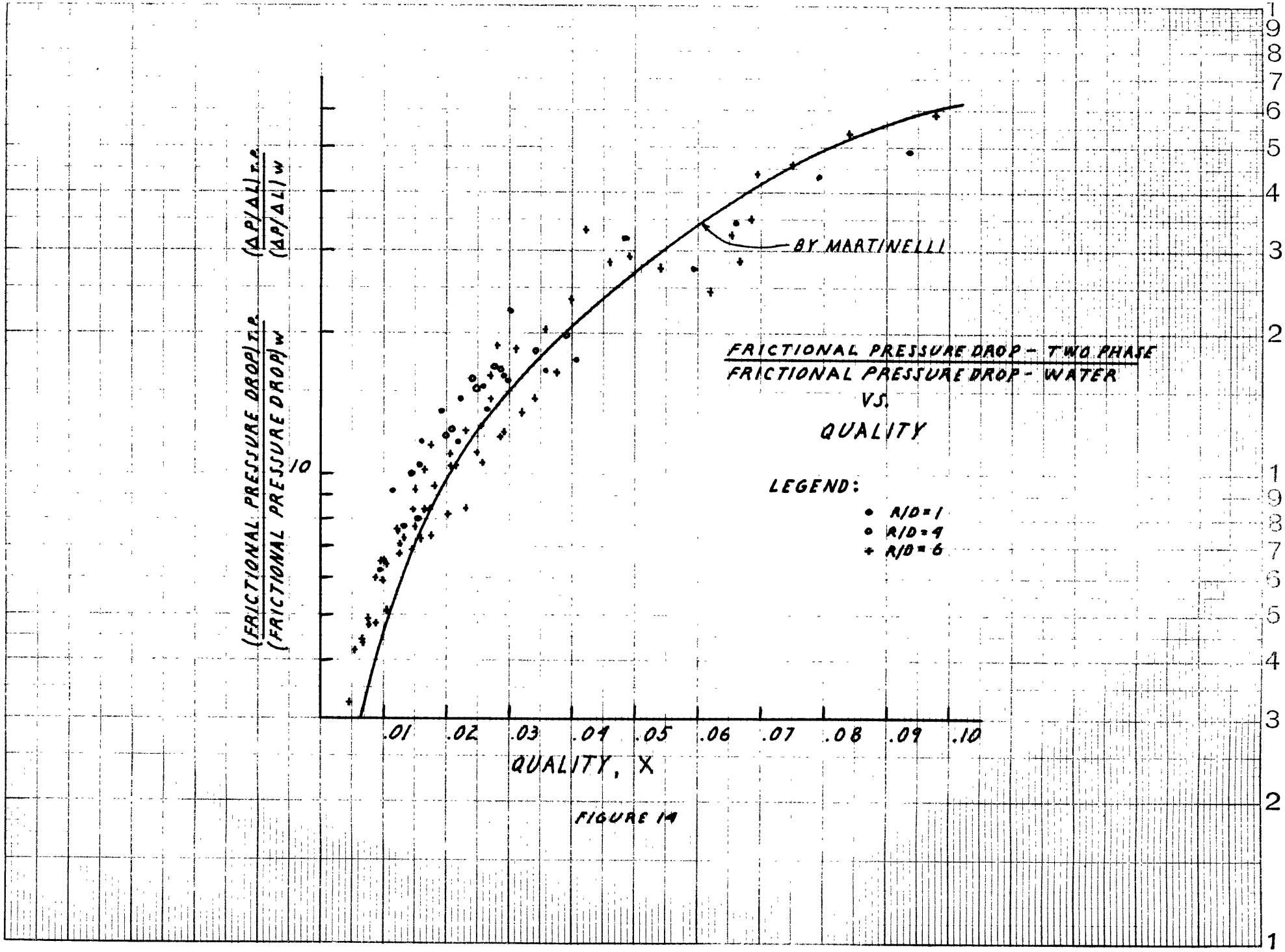
(FRICTIONAL PRESSURE DROP)T.P. / (FRICTIONAL PRESSURE DROP)W
(ΔP/ΔL)T.P. / (ΔP/ΔL)W
10
BY MARTINELLI
FRICTIONAL PRESSURE DROP - TWO PHASE / FRICTIONAL PRESSURE DROP - WATER
VS.
QUALITY
LEGEND:
R/D = 1
R/D = 4
R/D = 6
.01
.02
.03
.04
.05
.06
.07
.08
.09
.10
QUALITY, X

FIGURE 14

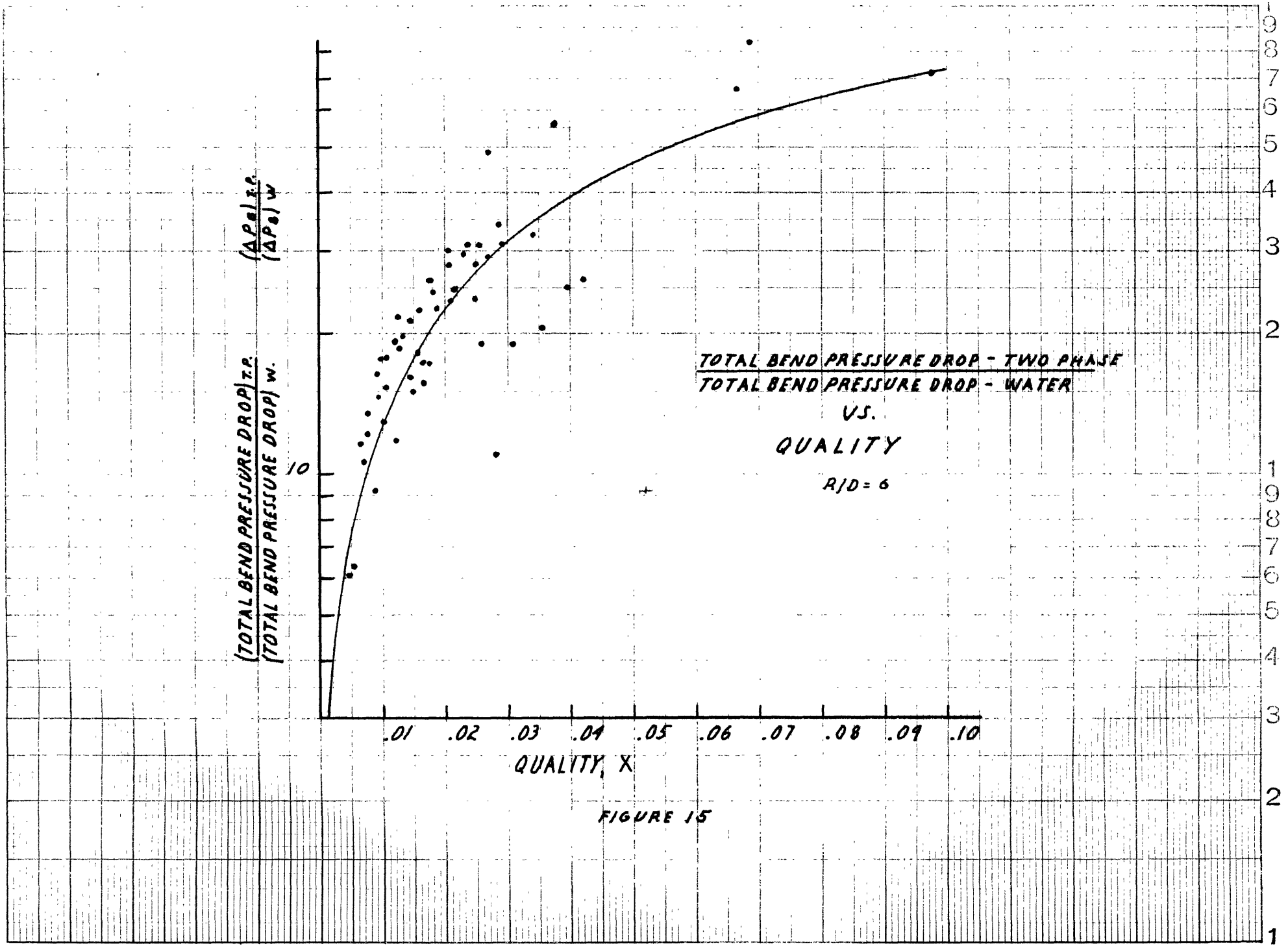
(TOTAL BEND PRESSURE DROP)T.P. / (TOTAL BEND PRESSURE DROP) W.
(ΔPe)T.P. / (ΔPe) W
10
.01
.02
.03
.04
.05
.06
.07
.08
.09
.10
QUALITY, X
TOTAL BEND PRESSURE DROP - TWO PHASE
TOTAL BEND PRESSURE DROP - WATER
VS.
QUALITY
R/D = 6

FIGURE 15

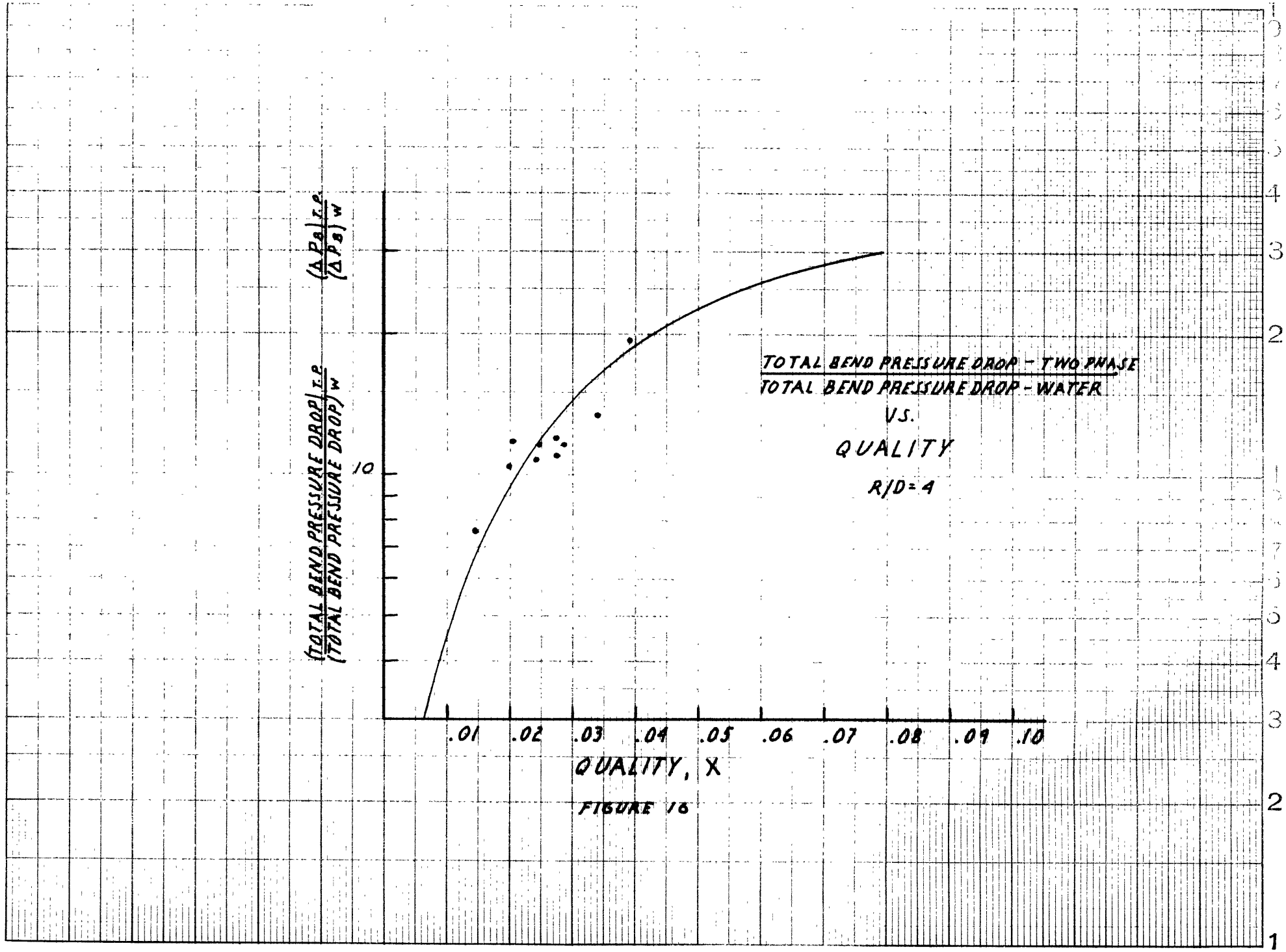
(TOTAL BEND PRESSURE DROP)$_{T.P.}$ / (TOTAL BEND PRESSURE DROP)$_{W}$
(ΔPa)$_{T.P.}$ / (ΔPa)$_{W}$
10
TOTAL BEND PRESSURE DROP - TWO PHASE / TOTAL BEND PRESSURE DROP - WATER
VS.
QUALITY
R/D = 4
.01
.02
.03
.04
.05
.06
.07
.08
.09
.10
QUALITY, X

FIGURE 16

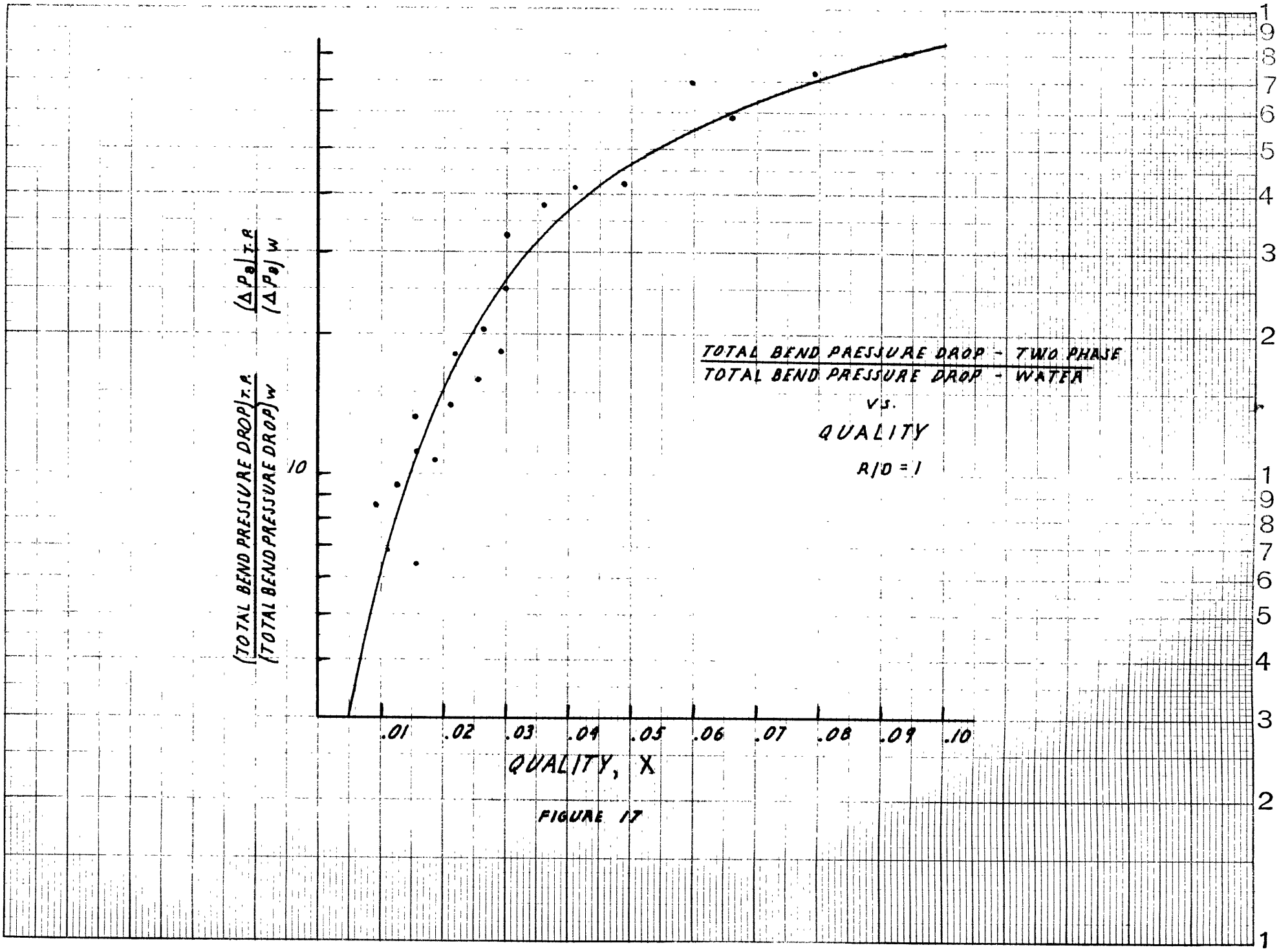
(TOTAL BEND PRESSURE DROP)T.P. / (TOTAL BEND PRESSURE DROP)W
(ΔPB)T.P / (ΔPB)W
10
TOTAL BEND PRESSURE DROP - TWO PHASE
TOTAL BEND PRESSURE DROP - WATER
VS.
QUALITY
R/D = 1
.01
.02
.03
.04
.05
.06
.07
.08
.09
.10
QUALITY, X

FIGURE 17

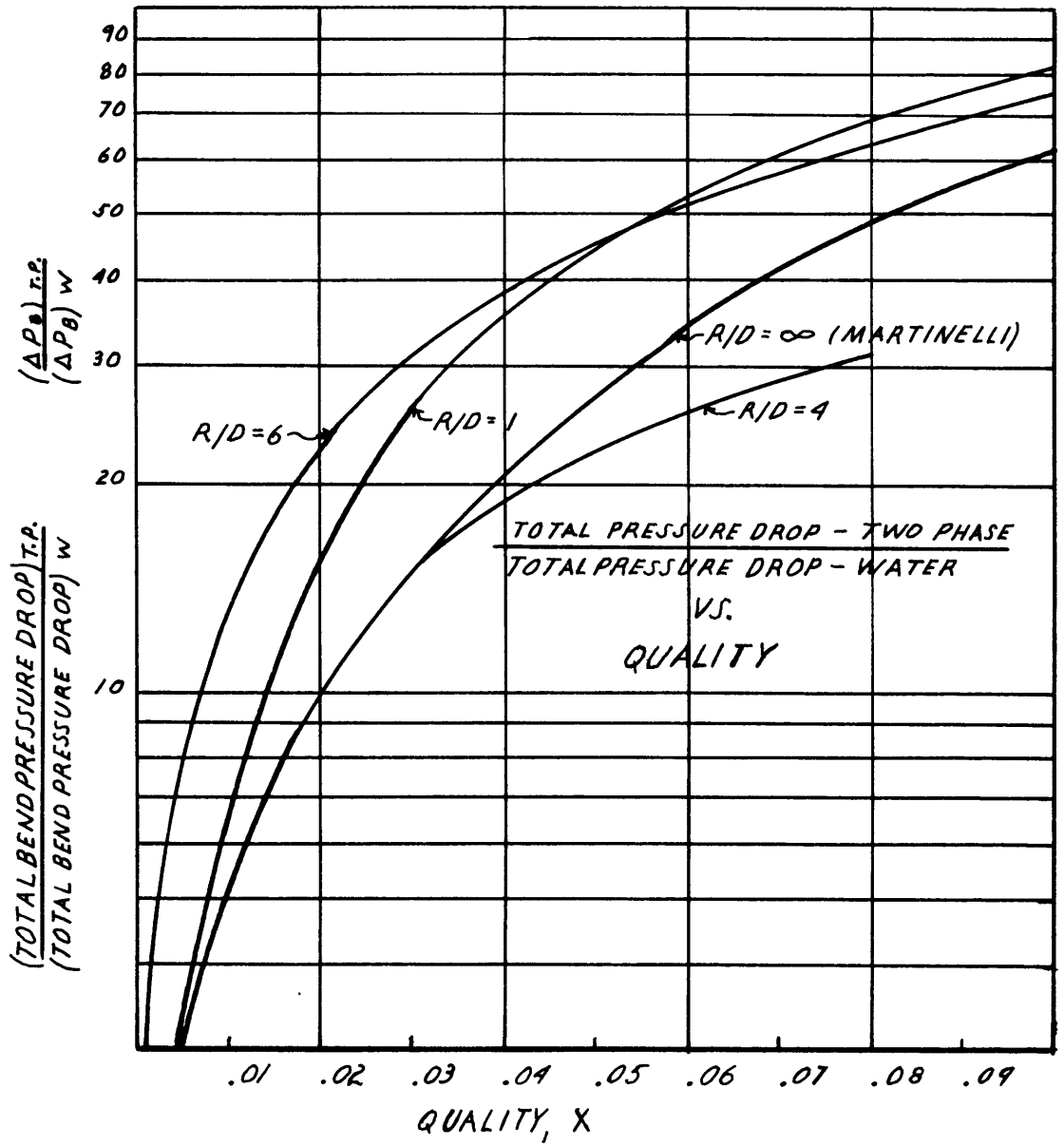
90
80
70
60
50
40
30
20
10
$\left(\frac{\Delta P_B)_{T.P.}}{(\Delta P_B)_W}\right.$
$\left.\frac{(TOTAL\ BEND\ PRESSURE\ DROP)_{T.P.}}{(TOTAL\ BEND\ PRESSURE\ DROP)_W}\right.$
R/D = 6
R/D = 1
R/D = ∞ (MARTINELLI)
R/D = 4
TOTAL PRESSURE DROP - TWO PHASE
TOTAL PRESSURE DROP - WATER
VS.
QUALITY
.01
.02
.03
.04
.05
.06
.07
.08
.09
QUALITY, X

FIGURE 18

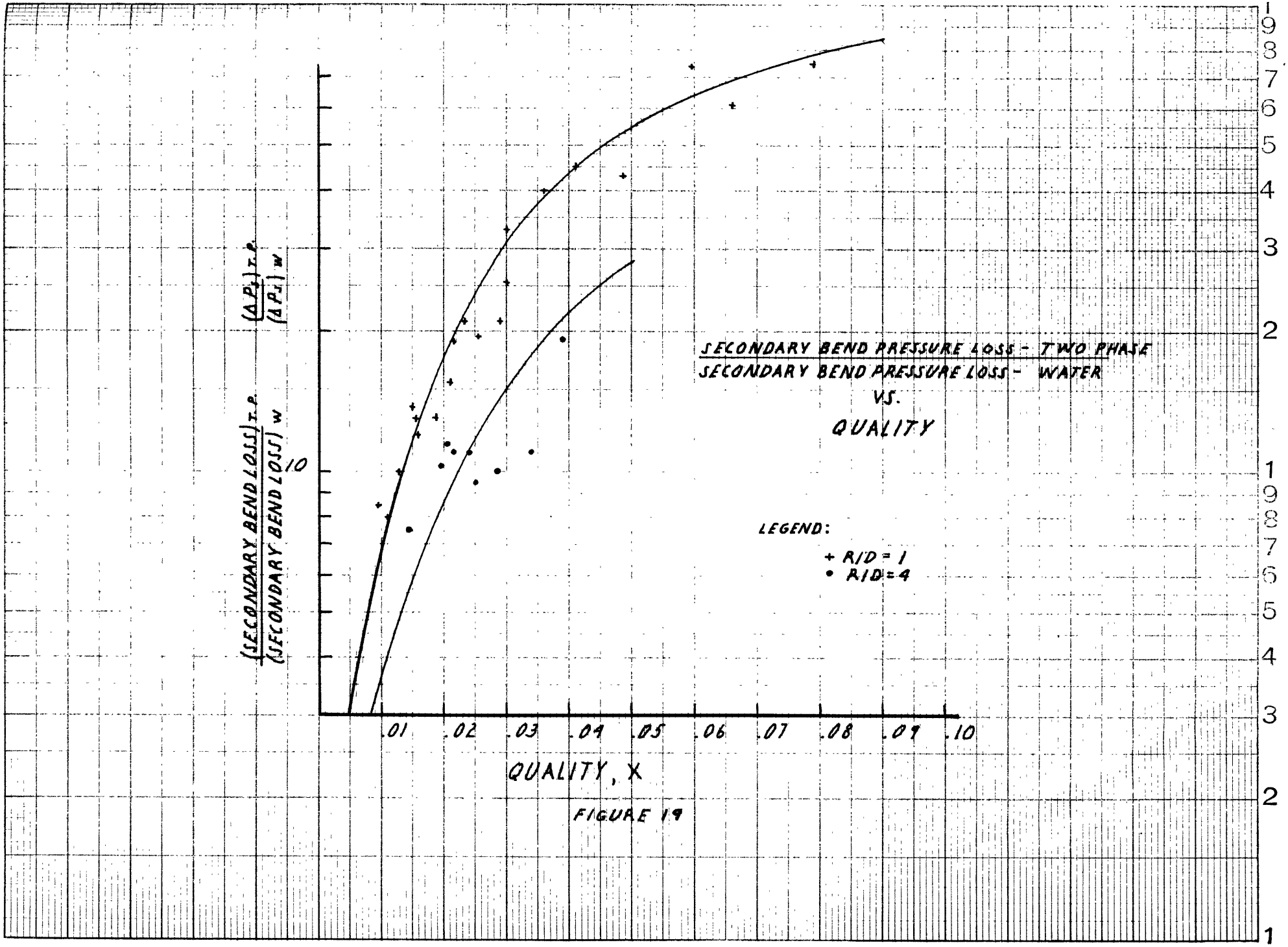
(SECONDARY BEND LOSS)T.P. / (SECONDARY BEND LOSS)W
(ΔP2)T.P. / (ΔP2)W
10
SECONDARY BEND PRESSURE LOSS - TWO PHASE / SECONDARY BEND PRESSURE LOSS - WATER
VS.
QUALITY
LEGEND:
+ R/D = 1
• R/D = 4
.01
.02
.03
.04
.05
.06
.07
.08
.09
.10
QUALITY, X

FIGURE 19

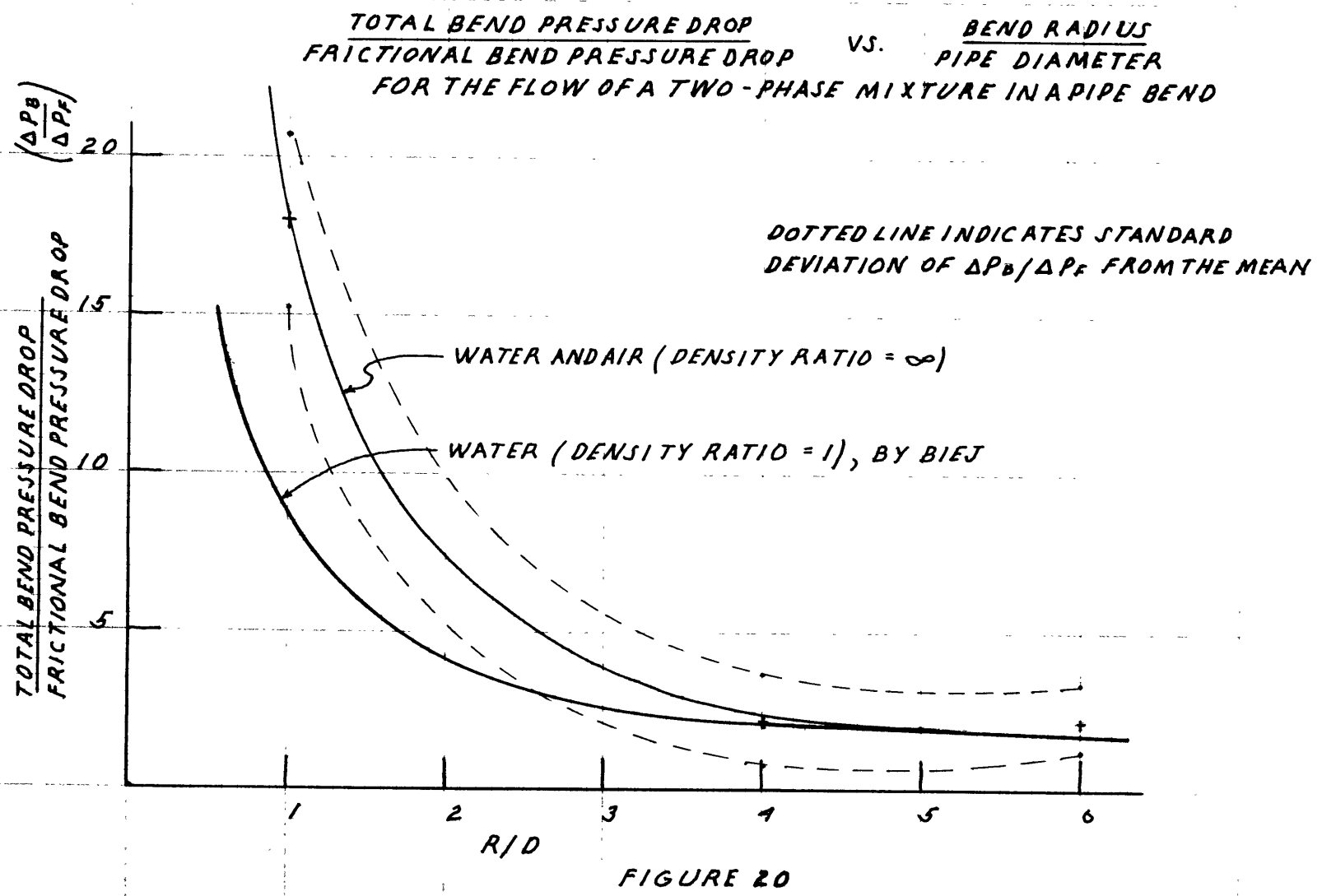
TOTAL BEND PRESSURE DROP / FRICTIONAL BEND PRESSURE DROP VS. BEND RADIUS / PIPE DIAMETER
FOR THE FLOW OF A TWO-PHASE MIXTURE IN A PIPE BEND
DOTTED LINE INDICATES STANDARD DEVIATION OF ΔPB/ΔPF FROM THE MEAN
WATER AND AIR (DENSITY RATIO = ∞)
WATER (DENSITY RATIO = 1), BY BIEJ
TOTAL BEND PRESSURE DROP / FRICTIONAL BEND PRESSURE DROP (ΔPB/ΔPF)
20
15
10
5
1
2
3
4
5
6
R/D

FIGURE 20

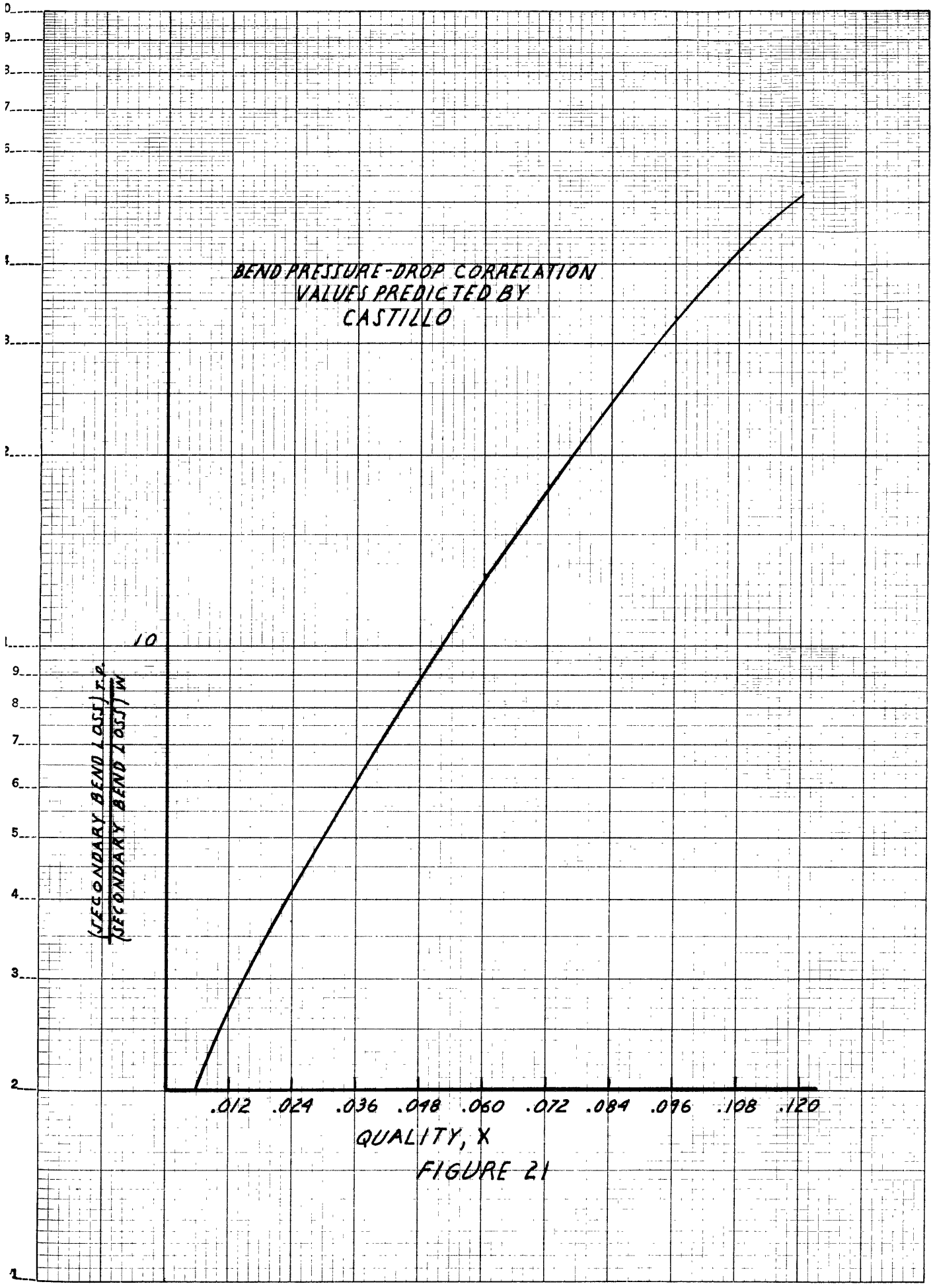
BEND PRESSURE-DROP CORRELATION
VALUES PREDICTED BY
CASTILLO
10
(SECONDARY BEND LOSS) r.p.
(SECONDARY BEND LOSS) W
.012
.024
.036
.048
.060
.072
.084
.096
.108
.120
QUALITY, X

FIGURE 21

APPENDIX IV

NOMENCLATURE

A	crossectional area of pipe, $in.^2$
D	inside pipe diameter, in.
f	Fanning friction factor
G	mass velocity, $lb/sec\text{-}ft^2$
H	pressure, inches of fluid
K	nozzle coefficient
K_o	radius of gyration
L	length of straight pipe, in.
g	gravitational constant, ft/sec^2
R	mean bend radius
R/D	relative bend radius
R_e	Reynolds number
V	mean fluid velocity, ft/sec
w	mass flow rate, lb/sec
x	quality, percent vapor by mass
P	pressure, psia
$\alpha, \beta, \chi, \Phi$	Martinelli parameters
ρ	density, lb/sec^2
ϵ, Λ	bend loss coefficients
η	bend loss coefficient, equals $\epsilon + \Lambda$

Subscripts

f	friction
g	gas flow
l	liquid flow
o	when the total flow is a liquid
tt	when both phases are turbulent

APPENDIX V

BIBLIOGRAPHY

1. O. Baker, Simultaneous Flow of Oil and Gas, Oil and Gas Journal, July 24, 1954.

2. R. C. Martinelli, L. M. H. Boelter, T. H. M. Taylor, E. G. Thomsen and E. H. Morrin, Isothermal Pressure Drop for Two-Phase Two-Component Flow in a Horizontal Pipe, Trans. Am. Soc. Mech. Eng., Feb., 1944.

3. K. H. Biej, Pressure Losses for Fluid Flow in 90° Pipe Bends, Journal of Res. of the Nat. Bur. of Standards, Vol. 21, July, 1938.

4. J. Castillo, A Study of Two-Phase Flow in Bends, S. M. Thesis, M.I.T., June, 1957.

5. L. F. Moody, Friction Factors for Pipe Flow, Trans. Am. Soc. Mech. Eng., Vol. 66, 1944.

6. D. Strawson, A Study of the Interface of a Two-Phase Stratified Flow, S. B. Thesis, M.I.T., June, 1957.

7. Am. Soc. of Mech. Eng., Power Test Codes, 1949.